Journal of the American Heart Association

ORIGINAL RESEARCH

Role of Maternal Obesity in Offspring Cardiovascular Development and Congenital Heart Defects

Ashleigh McMullan, MS*; James B. Zwierzynski, MS*; Nina Jain; Laura S. Haneline, MD; Weinian Shou, PhD; Kok Lim Kua, MD; Swetansu K. Hota, PhD; Matthew D. Durbin, MD

BACKGROUND: Congenital heart disease is a leading cause of death in newborns, yet many of its molecular mechanisms remain unknown. Both maternal obesity and diabetes increase the risk of congenital heart disease in offspring, with recent studies suggesting these conditions may have distinct teratogenic mechanisms. The global prevalence of obesity is rising, and while maternal obesity is a known risk factor for fetal congenital heart disease, the specific mechanisms are largely unexplored.

METHODS AND RESULTS: We used a murine model of diet-induced maternal obesity, without diabetes, to produce dams that were overweight but had normal blood glucose levels. Embryos were generated and their developing hearts analyzed. Transcriptome analysis was performed using single-nucleus and bulk RNA sequencing. Global and phospho-enriched proteome analysis was performed using tandem mass tag–mass spectroscopy. Immunobloting and histologic evaluation were also performed.

Analysis revealed disrupted oxidative phosphorylation and reactive oxygen species formation, with reduced antioxidant capacity, evidenced by downregulation of genes *Sod1* and *Gp4x*, and disrupted *Hif1a* signaling. Evidence of oxidative stress, cell death signaling, and alteration in Rho GTPase and actin cytoskeleton signaling was also observed. Genes involved in cardiac morphogenesis, including *Hand2*, were downregulated, and fewer mature cardiomyocytes were present. Histologic analysis confirmed increased cardiac defects in embryos exposed to maternal obesity.

CONCLUSIONS: These findings demonstrate that maternal obesity alone can result in cardiac defects through mechanisms similar to those associated with maternal hyperglycemia. This study provides valuable insight into the role of maternal obesity, a growing and modifiable risk factor, in the development of the most common birth defect, congenital heart disease.

Key Words: cardiac development ■ congenital heart disease ■ gene–environment interaction ■ maternal obesity

Congenital heart disease (CHD) is the most common birth defect, occurring in approximately 1% of live births. CHD is also the leading cause of birth defect–related death, responsible for 4.2% of all neonatal deaths.[1–4] Despite the prevalence and significant disease burden, many of the developmental pathways and molecular mechanisms contributing to CHD pathogenesis remain unknown.[5] Approximately 30% of CHD cases can be attributed to direct genetic determinants including chromosomal aneuploidy, copy number variants and de novo mutations.[6,7] In addition to direct genetic causes, epidemiological studies demonstrate that CHD is underpinned by environmental factors, as well as multifactorial inheritance, including gene–environment

Correspondence to: Matthew D. Durbin, MD MS, Herman B. Wells Center for Pediatric Research, 1044 W. Walnut, R4 221, Indianapolis, IN 46202-5225. Email: mddurbin@iu.edu

*A. McMullan and J. Zwierzynski contributed equally.

This manuscript was sent to June-Wha Rhee, MD, Associate Editor, for review by expert referees, editorial decision, and final disposition.

Preprint posted on SSRN July 22, 2024. https://doi.org/10.2139/ssrn.4898984.

Supplemental Material is available at https://www.ahajournals.org/doi/suppl/10.1161/JAHA.124.039684

For Sources of Funding and Disclosures, see page 17.

JAHA is available at: www.ahajournals.org/journal/jaha

RESEARCH PERSPECTIVE

What Is New?

- This study provides valuable insight into the role of maternal obesity in offspring development of the most common birth defect, congenital heart disease.
- The results highlight that maternal obesity alone can result in cardiac defects in offspring through mechanisms similar to those seen in maternal diabetes, including reduced antioxidant capacity, oxidative stress, cell death signaling, alterations in Rho GTPase and actin cytoskeleton signaling, and a reduced number of mature cardiomyocytes, leading to offspring septal defects.

What Question Should Be Addressed Next?

- Obesity can be managed through lifestyle changes, surgical interventions, and emerging pharmaceuticals, and antioxidant therapies may hold promise for preventing congenital heart disease; however, a recent study in mice suggests that genetic factors may influence response to these therapies; future studies should focus on a deeper mechanistic analysis of maternal obesity's role in offspring congenital heart disease, potentially leading to tailored therapeutic and preventative strategies to reduce the occurrence and severity of congenital heart disease.

Nonstandard Abbreviations and Acronyms

8-OHdG	8-hydroxy-2′-deoxyguanosine
EIF	eukaryotic initiation factor
FDR	false discovery rate
GTT	glucose tolerance testing
IPA	ingenuity pathway analysis
ITT	insulin tolerance testing
mTOR	mechanistic target of rapamycin
ROCK	Rho-associated coiled-coil containing protein kinase
ROS	reactive oxygen species
snRNAseq	single-nucleus RNA sequencing
TMT-MS	tandem mass tag–mass spectroscopy
WNT/PCP	noncanonical Wnt/planar cell polarity

interactions during embryogenesis.[8] Investigation into these gene–environment interactions is necessary to understand the pathogenesis of CHD and develop targeted therapeutic and preventative strategies.

Several environmental factors are associated with an increased risk of CHD in offspring, including maternal medications, infections, diabetes, and obesity.[8] A number of studies demonstrate a significant association between CHD in offspring and maternal obesity as a primary modifiable risk factor.[9–14] Worldwide, rates of obesity have doubled since 1990 in the general population, and rates have quadrupled in adolescents, which is of particular concern given the proximity to reproductive age.[15] Though maternal obesity correlates with CHD, the mechanisms remain unknown.

Epidemiologic studies demonstrate that maternal obesity is associated with a range of offspring complex CHDs.[16–19] These studies also indicate a dose–response relationship, with the severity of maternal obesity correlating to CHD risk.[18,19] Maternal obesity and maternal diabetes are often grouped together and considered on the same spectrum; however, a recent epidemiologic study demonstrates different risk profiles, with differential rates of CHD types between diabetes and obesity, suggesting distinct underlying teratogenic mechanisms.[16] While studies have examined the mechanism of CHD due to maternal diabetes, including the role of oxidative stress and reduced antioxidant capacity,[20–25] the mechanism of CHD due to maternal obesity remains largely unexplored.

Here, we use a diet-induced maternal obesity murine model to investigate the associated risk of congenital cardiac anomalies in offspring. We use complementary multiomics and histologic analysis to examine the corresponding cellular, transcriptional, proteomic, and histologic changes in the developing murine heart.

METHODS

Material Availability

This study did not generate new unique reagents.

Data Availability

All data are deposited in data type-specific repositories; all transcriptomics data have been uploaded to Gene Expression Omnibus and all proteomics data have been uploaded to the ProteomeXchange Consortium via the PRIDE partner repository with the dataset identifier PXD062087 and 10.6019/PXD062087. All data are available upon request to the lead contact.

Diet-Induced Maternal Obesity Model

Wild-type C57BL/6J mice or *Shroom3*^{gt} mice were acquired from Jackson Laboratory (Bar Harbor, Maine; Nos. 000664, 003754). At 5 weeks old, mice were randomly assigned to either a regular chow with 18 kcal% fat (2018SX; Inotiv, Indianapolis, IN) as a control or a rodent diet with 60 kcal% fat (Table S1; D12492;

Research Diets Inc., New Brunswick, NJ), to induce maternal obesity. We designed the study in consultation with the Indiana University Diabetes Core, to generate twice the number of high-fat dams, given that the proinflammatory state of obesity induces subfertility in mice, with the tendency of obesity to decrease the pregnancy rate as well as litter size.[26] Female mice underwent EchoMRI (EchoMRI LLC, Houston, TX) body composition evaluation and nonfasting blood glucose measurements at week 5 and week 9. A separate cohort of mice was used for model assessment and underwent fasting blood glucose measurement along with glucose tolerance testing (GTT) and insulin tolerance testing (ITT) at week 9. For the GTT, mice were fasted for 4 hours, then 1 g/kg of glucose was injected intraperitoneally, and blood was collected via tail biopsy at 0, 10, 20, 30, 60, and 90 minutes. For ITT, mice were fasted for 2 hours, and then 0.75 U/kg of Humulin R (Elly Lilly, Indianapolis, IN) was administered intraperitoneally, and blood glucose was measured at 0, 15, 30, 45, and 60 minutes. All glucose measurements were taken via tail biopsy using an Alphatrak II Glucometer (Zoetis Petcare, Parsippany, NJ). Model assessments, including EchoMRI, glucose monitoring, GTT, and ITT, were completed by the Indiana University Diabetes Core. After measurements at 9 weeks, females were mated with male mice on a regular chow diet. Gestational age was determined by checking for the presence of a vaginal plug with the date of sperm plug observation representing embryonic day 0.5 of development. Pregnant females were maintained on respective diets throughout gestation. Animal handlings were carried out within the Indiana University School of Medicine Animal Resource Center accredited by the American Association for Accreditation of Laboratory Animal Care. Ethical approval was granted by the Institutional Animal Care and Use Committee (Protocol Number 21159). Animals were appropriately housed in a temperature-controlled environment, in 12-hour light–dark cycles, with continual access to food and water. We used the Animal Research: Reporting of In Vivo Experiments reporting checklist.[27]

E12.5 Wild-Type Embryonic Heart Retrieval

At embryonic day 12.5, wild-type dams on respective diets were euthanized using carbon dioxide. Embryonic day 12.5 embryos were harvested; hearts were further micro-dissected, and flash frozen immediately upon dissection. A total of 13 embryonic hearts were harvested respectively from high-fat (n=13) and control (n=13) groups for multiomic analysis including bulk RNA sequencing, tandem mass tag–mass spectroscopy (TMT-MS), single-nucleus RNA sequencing (snRNAseq), and immunoblot. Limb bud tissue was additionally harvested during each embryonic heart tissue retrieval for sex genotyping.

Single-Nucleus RNA Sequencing

Embryonic day 12.5 embryonic hearts were harvested and flash frozen from high-fat (n=5) and control (n=5) dams for snRNAseq analysis. Embryonic hearts were litter matched and sex matched, and high-fat (n=5) hearts were pooled in one tube and control (n=5) hearts were pooled in another. Nuclei isolation and snRNAseq was performed by Singulomics Corporation (Bronx, NY). Briefly, heart tissue was homogenized and lysed with Triton X-100 in RNase-free water for nucleus isolation. Isolated nuclei were purified, centrifuged, and resuspended in PBS with RNase inhibitor, then diluted to 700 nuclei/μL for standardized 10x Genomics capture and library preparation protocol with 10x Genomics Chromium Next GEM 3′ Single Cell Reagent kits version 3.1 (10x Genomics, Pleasanton, CA). Libraries were sequenced with NovaSeq 6000 (Illumina, San Diego, CA). Raw sequencing files were processed with CellRanger 6.0 (10x Genomics). Sequences were mapped to the *Mus musculus* genome (mm10), including introns to generate gene count matrices. Downstream analysis was performed with Seurat 4.0. For all samples, nuclei were filtered out with <200 genes and >5% mitochondrial genes. The final filtered matrix for samples contained 7015 nuclei and 23 949 genes. Cell-type clustering was performed using canonical markers for cardiac cell types.

Bulk RNA Sequencing

Embryonic day 12.5 embryonic hearts were harvested and flash frozen from high-fat (n=4) and control (n=4) dams for bulk RNA sequencing analysis. Total RNA was harvested from flash-frozen hearts using the RNeasy Plus Mini Kit (ID: 74134; Qiagen, Hilden, Germany). Litter-matched and sex-matched flash-frozen embryonic hearts were used. One hundred nanograms of eluted RNA was prepared using KAPA mRNA, and sequencing libraries were generated, sequenced, and results were bioinformatically compared in collaboration with Indiana University Center for Medical Genomics and Bioinformatics Core using an Illumnia NovaSeq6000 at 2×250 bp read length to compare differential expression. An average of 42 million high-quality reads were generated for pooled control and an average of 39 million high-quality reads were generated for pooled high-fat heart samples.

Tandem Mass Tag–Mass Spectrometry

Embryonic day 12.5 embryonic hearts were harvested and flash frozen from high-fat (n=4) and control (n=4) dams for TMT-MS analysis. Litter-matched and sex-matched flash-frozen embryonic hearts were transferred using 100 μL of 8M urea, then lysed with mechanical disruption by pipetting. Bioruptor (Diagenode, Denville, NJ) sonication of 30 cycles (30 seconds on/30 seconds off schedule) yielded ≈60 μg of protein from each group. The peptides were desalted on Sep-Pak (Waters, Milford, MA), yielding ≈50 μg of protein. Proteins were TMT-labeled using TMTpro (A44520, Lot WC320807; Thermo Fisher Scientific, Waltham, MA), using 0.5 mg of reagent for each global sample; after quenching, the samples were mixed, dried, and desalted on 100 mg Sep-Pak Columns (Waters). Samples were enriched for phosphopeptides using High Select TiO2 Phosphopeptide Enrichment Kit (A32993; Thermo Fisher Scientific). Phosophopeptides were eluted from the kit. High-pH solvent-based fractionation of peptides was used to fractionate one third of the global peptides on a 50-mg Sep-Pak Column (Waters), followed by liquid chromatography–tandem mass spectrometry. One fifth of each global sample and one half of each phosphopeptide sample was injected and run on the Eclipse Orbitrap Mass Spectrometer (Thermo Fisher Scientific). Data were analyzed against the UniProt Mus musculus protein database using Proteome Discoverer Software version 2.5 (Thermo Fisher Scientific). Results were filtered for high-confidence peptides, FASTA files with common contaminants were added to the protein marker node, and quantitative abundances were normalized to the same total peptide amount per channel so that average abundance per peptide and protein was 100. Sample preparation, protein and phosphoprotein isolation, mass spectrometry analysis, bioinformatics and data evaluation for quantitative proteomic and phosphoproteomic experiments was performed in collaboration with the Indiana University School of Medicine Center for Proteome Analysis similar to previously published protocols and more detailed methods are available (Data S1).[28,29]

Immunoblot Analysis

Embryonic day 12.5 embryonic hearts were harvested and flash-frozen from high-fat (n=4) and control (n=4) dams for immunoblot analysis. Flash-frozen hearts were lysed in RIPA Lysis and Extraction buffer (Thermo Fisher Scientific), supplemented with HALT Protease and Phosphatase Inhibitor (Thermo Fisher Scientific), and homogenized with BeadBug microtube tissue homogenizer (Benchmark Scientific, Edison, NJ). A subset of lysate was used for protein quantification with Pierce BCA Protein assay (Thermo Fisher Scientific). Equal amounts of protein lysate for each sample were mixed 3 to 1 with Laemmli loading buffer (Promega, Madison, WI), denatured, and electrophoresed on novex wedgewell polyacrylamide gels (Thermo Fisher Scientific) and transferred to nitrocellulose membranes (Bio-Rad Laboratories, Hercules, CA). Protein underwent immunoblot analysis using antibodies for 8-hydroxy-2′-deoxyguanosine (8-OHdG; Thermo Fisher; bs-1278R), total cofilin (Cell Signaling Technology, Danvers, MA; No. 5175) phosphorylated cofilin (Cell Signaling Technology; No. 3313) and GAPDH (Abcam, Cambridge, UK; ab9485). The nitrocellulose membranes were cut into target strips and probed with antibody for GAPDH, phosphorylated cofilin or 8-OHdG, followed by stripping the blot using Restore WB Stripping Buffer (Thermo Fisher Scientific), reblocking the membrane, and then reimmunoblotting with antibody for total cofilin or GAPDH and immunoblots were quantified in Image J and analyzed with a Mann–Whitney statistical analysis in Prism 10 (GraphPad Software, La Jolla, CA).

Histological Analysis

Embryos were collected at embryonic day 14.5, after the intraventricular septum had closed during normal development. Genotyping was carried out using genomic DNA extracted from ear punches, embryonic tissue, or yolk sacs. The genotyping for *Shroom3* was performed using polymerase chain reaction for β-galactosidase (5′-AACTTAATCGCCTTGCAGCA-3′ and 5′-GTAACCGTGCATCTGCCAGT-3′) and a wild-type allele (5′-GGCCCCAGACTCACCATAATC-3′ and 5′-GCAACCACATGGTGGCTCACAAGC-3′). Following fixation in 4% (v/v) paraformaldehyde, the embryos were dehydrated, paraffin embedded, and transversely sectioned at 5 μm. The sections were stained with hematoxylin and eosin (Sigma-Aldrich, Burlington, MA) and examined under a microscope to identify cardiac defects. Each slide was reviewed by 2 independent, blinded reviewers, and any discrepancies in identifying cardiac defects were resolved by a third blinded party. The resulting genotypes and cardiac defects were compared with expected Mendelian ratios and between high-fat and control diet groups, using χ^2 analyses. Figures were created with the assistance of Biorender.

Statistical Analysis

Single time-point measurements assessing body composition data between groups used a Student's 2-tailed *t* test. We performed pathway enrichment using ShinyGo[30] and ingenuity pathway analysis (IPA) (Qiagen) for differentially expressed genes, proteins, and phosphoproteins (P<0.05). Statistical analyses were performed using Prism 10. P values <0.05 were considered statistically significant.

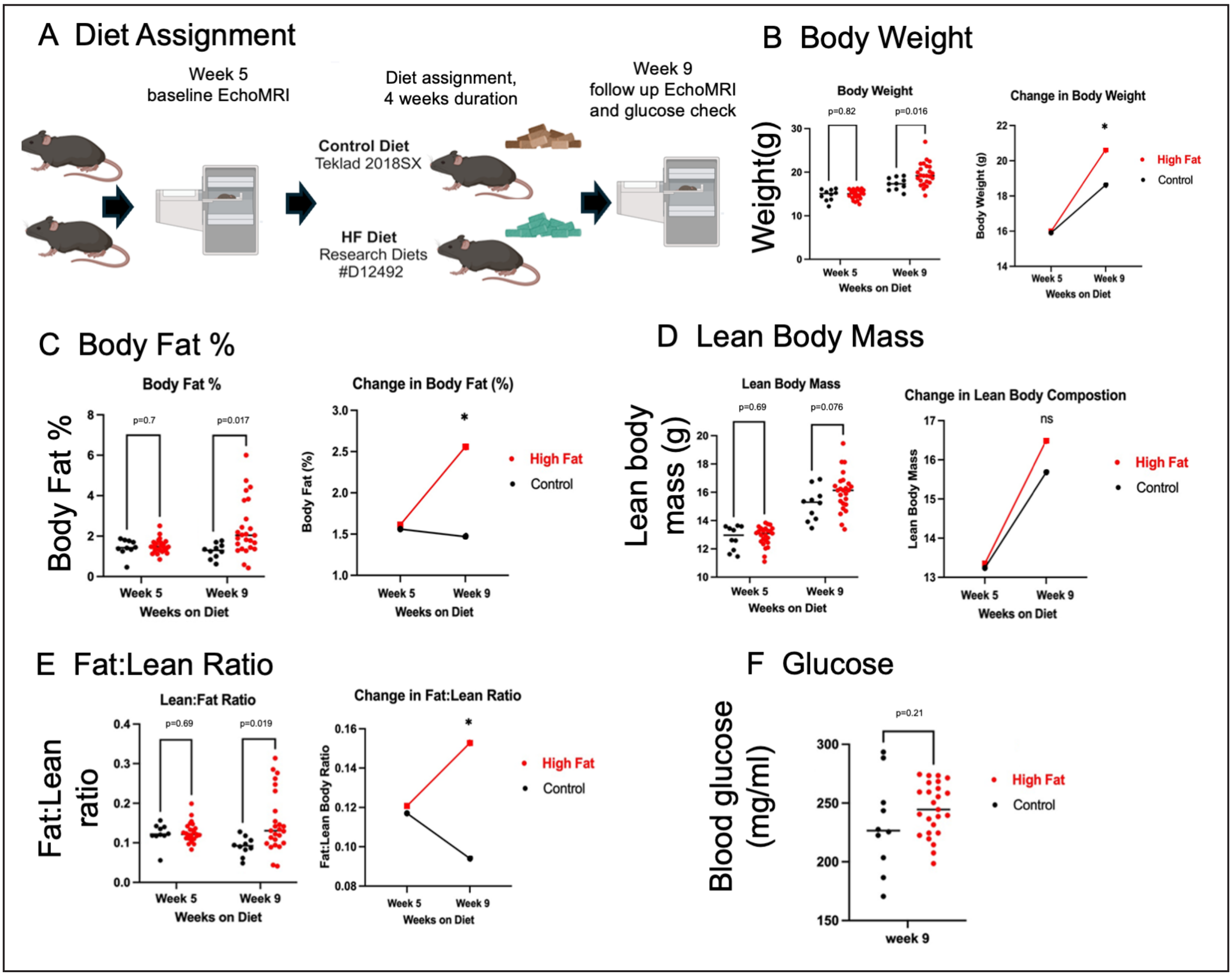

Figure 1. Diet-induced maternal obesity mouse model establishment (A).
Schematic timeline of experimental set up. EchoMRI body composition analysis comparison of maternal high-fat (n=25) and control (n=10) mice concerning (**B**). Total body weight at week 5 (P=0.82) and week 9 (P=0.016); (**C**) body fat (%), at week 5 (P=0.7) and week 9 (P=0.017); (**D**) lean body mass at week 5 (P=0.69) and week 9 (P=0.076); (**E**) fat:lean ratio at week 5 (P=0.69) and week 9 (P=0.019); and (**F**) blood glucose (mg/mL) at week 9 (P=0.21). HF indicates high-fat. *P<0.05; ns, P>0.05; and not significant.

RESULTS

Body Composition Analysis Via EchoMRI Confirmed Diet-Induced Maternal Obesity Model Establishment

We used diet-induced maternal obesity to investigate the impact of maternal obesity on offspring cardiac development. Female mice were placed on a high-fat or control diet at 5 weeks of age (Figure 1). Model establishment was confirmed by body composition analysis via EchoMRI at week 5 for baseline readings and then again at week 9 for assessment of obesity establishment in the respective diet cohorts (Figure 1A). At week 9, we observed that female mice on a high-fat diet gained significantly more weight compared with mice on a control diet (20.6 g versus 18.6 g, P=0.016; Figure 1B) Additionally, to confirm model establishment, we observed a significant difference in body fat percentage between high-fat and control cohorts at week 9 (2.5% versus 1.5%, P=0.017; Figure 1C). Further, in line with model establishment, we observed that lean body mass remained consistent between diet cohorts at both week 5 (P=0.672) and week 9 (16.5% versus 15.7%, P=0.076) on respective diets (Figure 1D). These data, in relation to a significant difference in total body weight between high-fat versus control females at week 9, indicates that overall maternal weight gain is secondary to a significant increase in body fat percentage. Further, this is supported by a significant difference observed in the measured fat-to-lean ratio between respective cohorts at week 9 (0.15 versus 0.094, P=0.019; Figure 1E). Following model establishment, blood glucose readings between diet cohorts taken at week 5 and week 9 displayed no significant change. At week 9, diet cohorts had no significant difference in blood glucose readings taken in a fed state (243 mg/mL versus 230 mg/mL, *P*=0.21; Figure 1F). In a In a fasting state, diet cohorts had slight but significant differences in GTT and ITT measurements at some time points but no difference in fasting blood glucose (fasting blood glucose: 170 versus 169, *P*=0.9203; GTT: 170 versus 169 at 0 minutes, 267 versus 304 at 10 minutes, 282 versus 341 at 20 minutes, 232 versus 327 at 30 minutes, 190 versus 233 at 60 minutes, and 169 versus 184 at 90 minutes, and ITT: 158 versus 161 at 0 minutes, 93 versus 113 at 15 minutes, 47 versus 71 at 30 minutes, 30 versus 49 at 45 minutes, 33 versus 48 at 60 minutes; Figure S1). Overall, primary body composition analysis and glucose readings taken between the 2 cohorts confirmed the establishment of diet-induced obesity, in line with previous publications,[31,32] with a demonstration of obesity, indicated by increased body weight and body fat composition, and despite some developing glucose intolerance, without glucose levels in the diabetic range, and with no significant difference in blood glucose levels in a fasting or fed state.

snRNAseq Analysis Reveals Significant Differences in the Abundance of Cardiac Cell Types Between Obesity Exposed and Control Embryo Hearts

To better understand maternal obesity–related transcriptional changes in the embryo heart, with single-cell resolution, we used in vivo 10x snRNAseq analysis (Figure 2). Wild-type C57BL/6J dams were placed on a high-fat or control diet from 5 weeks of life onward, and set up in timed mating after reaching 9 weeks of life, with a wild-type C57BL/6J male. We focused our assessment at embryonic day 12.5, at a time of active atrial, ventricular, and outflow tract septation, as offspring septal defects and outflow tract defects are attributed to maternal obesity in humans.[33] Embryos were harvested at embryonic day 12.5; the hearts were dissected and single nuclei isolated (Figure 2A). Single-cell libraries were obtained from the 10x Genomics Chromium system. Analysis from high-fat (n=5) and control (n=5) embryonic hearts captured a total of 7015 single nuclei with 3634 nuclei and 3381 nuclei captured, respectively (Figure 2B). Expression variability of all genes was subjected to nonlinear dimensionality reduction through uniform manifold approximation and projection, and 10 cell clusters were recognized (Figure 2C). Clusters were identified using expression of genes, including cardiomyocyte genes *Ryr2*, *Myocd*, and *Mhrt* (Figure 2D); endocardial genes *Nrg1* and *Emc* (Figure 2E); fibroblast genes *Postn*, *Robo2*, and *Unc5c* (Figure 2F); and epicardial genes *Tbx18* and *Wt1* (Figure 2G); additional genes were used to identify each cluster (Figure 2C). A shift in the distribution of cells in the obesity exposed compared with control embryo hearts was observed (Figure 2B and 2H). In obesity-exposed hearts, a decrease in cardiomyocyte cluster 1 and an increase in cardiomyocyte cluster 4 was detected. Cluster 1 represents more mature cardiomyocytes, expressing maturation markers such as *Ryr2*, *Slc8a1*, *Tnni3k*, *Fgf13*, *Myocd*, *Ttn*, *Palld*, *Dmd*, and *Myh6*, while cluster 4 cardiomyocytes are enriched in *Nppa*, *Tnni1*, *Acta2*, and *Myl4*, suggesting that these cells are immature, stressed, or developmentally delayed.

In addition, snRNAseq analysis found a decrease in fibroblasts and an increase in epicardial cells. There was also an increase in blood and immune cells. There was an upregulation of *Hba-a2* and *Hbb-bs* in obesity-exposed hearts, which were likely due to the presence of contaminating blood cells. Overall, this analysis suggests that maternal obesity disrupts embryo cardiac development, with changes in the distribution of multiple cell types important to cardiogenesis. Genes related to cardiac development were downregulated (Figure 2I) and upregulated (Figure 2J) in the total cell pool of developing hearts of embryos in the obesity-exposed group; however, given that the analysis used 1 pooled sample for each group, we did not have statistical power to identify differences in expression of individual genes. Therefore, we next performed bulk RNA sequencing analysis to identify differences in the expression of individual genes and identify pathways impacted (Figure 3).

Transcriptome Analysis Reveals Significant Differential Expression of Genes in Embryo Hearts Exposed to Maternal Obesity

To investigate transcriptome profiles of maternal obesity–exposed embryonic hearts, we used bulk RNA

Figure 2. SnRNAseq analysis of maternal obesity exposed and control embryo hearts.
A, Experimental design, with C57BL/6J females placed on high-fat or control diet from week 5 of life to week 9 of life, followed by a timed mating, embryo harvest at embryonic day 12.5, heart dissection from high-fat (n=5) and control (n=5) dams, followed by snRNAseq analysis. **B**, UMAP plot of 7015 single cells, with 3634 cells and 3381 cells captured for high-fat and control hearts, respectively. **C**, Ten cell types were identified. **D**, Feature plots with expression of cardiomyocyte genes, *Ryr2, Myocd*, and *Mhrt*. **E**, Expression of endocarial genes, *Nrg1* and *Emcn*. **F**, Expression of fibroblast genes, *Postn, Robo2*, and *Unc5c*. **G**, Expression of epicardial genes *Tbx18* and *Wt1*. **H**, Quantification of the number of cell types in high-fat and control embryonic hearts. **I**, Selected downregulated genes. **J**, Selected upregulated genes. **I** and **J** represent expression levels. The analysis used 1 pooled sample for each group and does not represent statistical differences in expression of the individual genes. HF indicates high-fat; snRNAseq, single-nucleus RNA sequencing; and UMAP, uniform manifold approximation and projection.

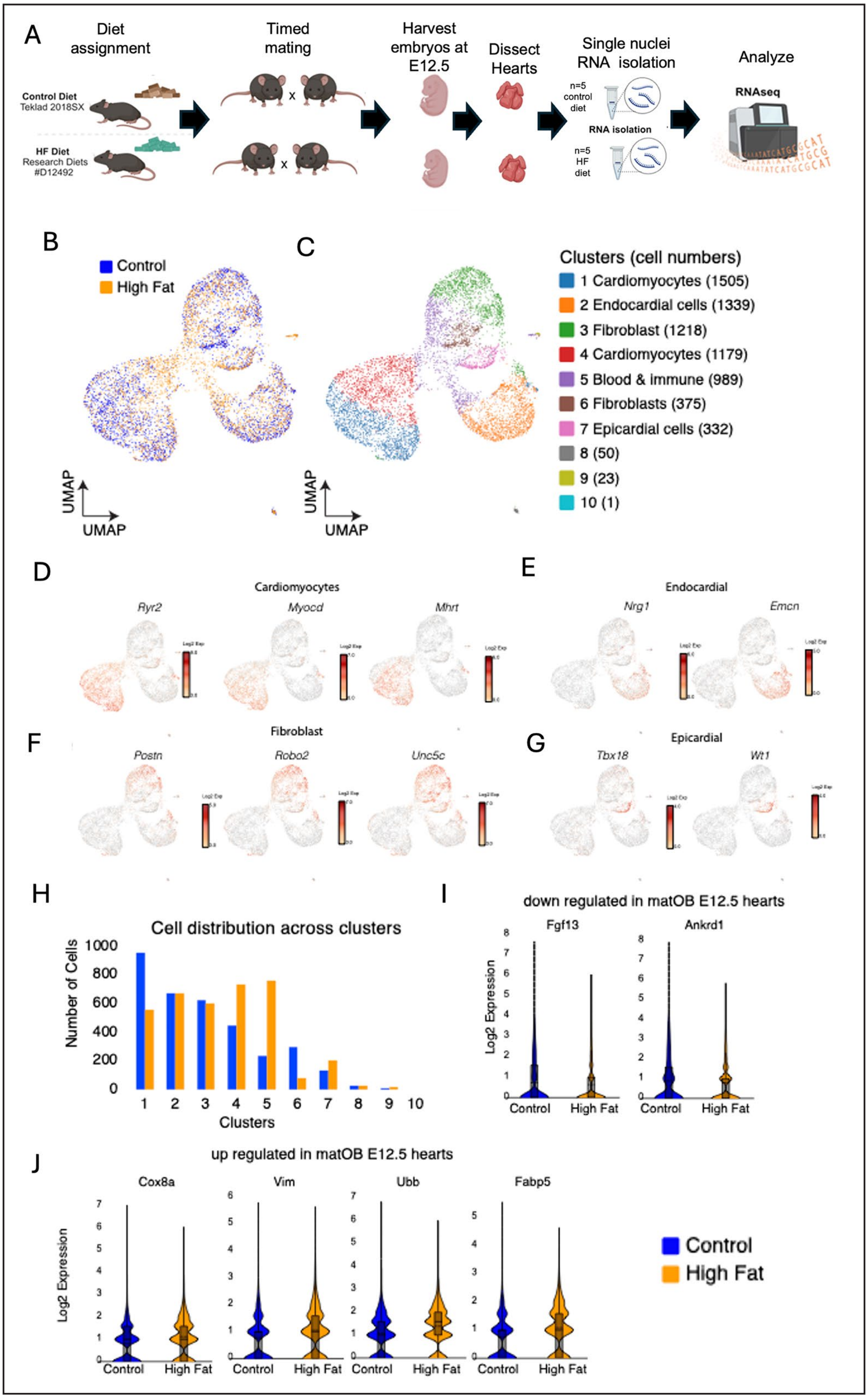

sequencing analysis on the obesity-exposed and control embryo hearts at embryonic day 12.5. Analysis of obesity-exposed embryonic hearts (n=4) versus control embryonic hearts (n=4) revealed 552 differentially expressed genes (false discovery rate [FDR] <0.05; Figure 3A and 3B), with the majority of genes

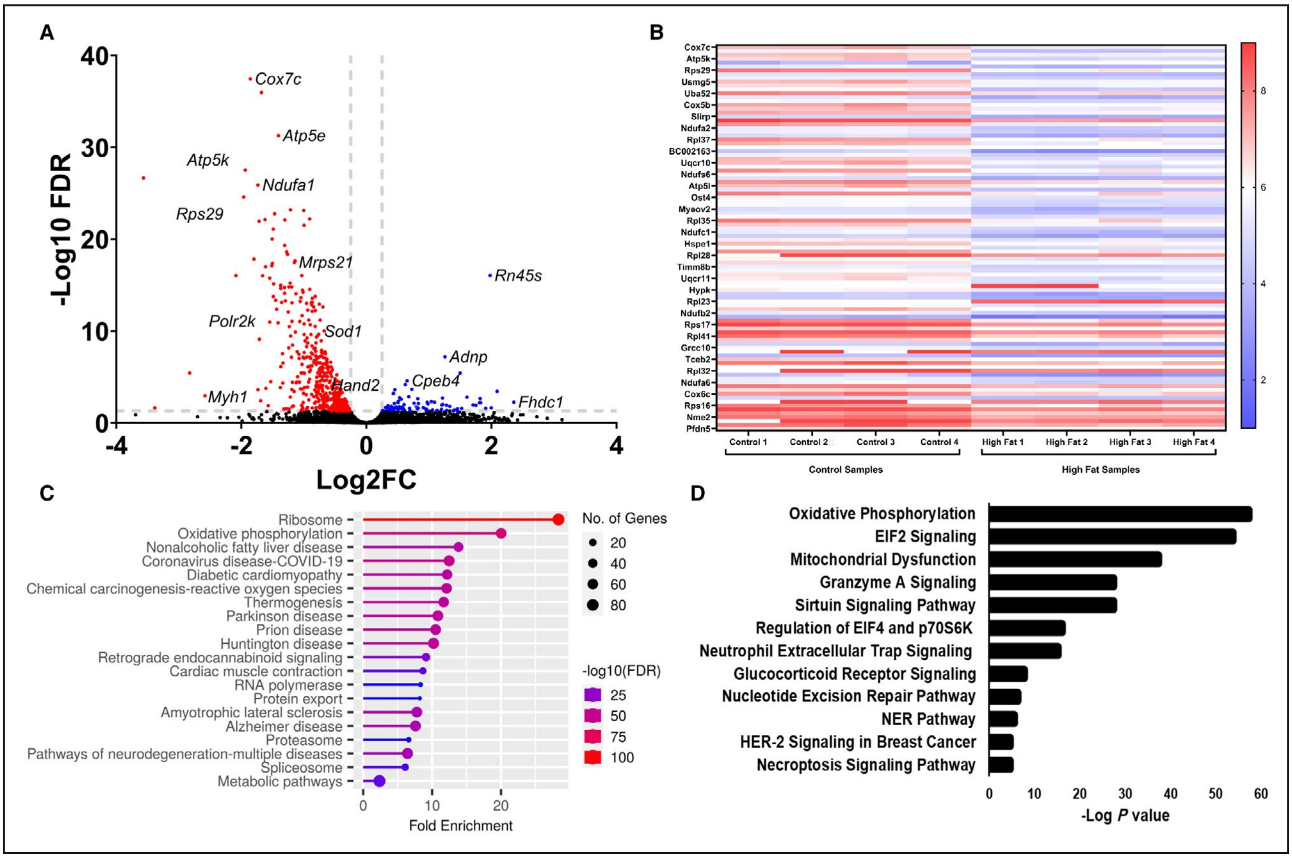

Figure 3. Transcriptome analysis of maternal obesity exposed and control embryonic hearts.
(**A**) RNA sequencing analysis of obesity-exposed (n=4) versus control (n=4) embryonic day 12.5 wild-type embryonic hearts, with a volcano plot depicting 552 significant differentially expressed genes observed between obesity-exposed versus control embryonic hearts (FDR <0.05). **B**, Heat map depicting top 100 significant differentially expressed gene between obesity-exposed and control groups with a random selection of 35 genes displayed (FDR <0.05). **C**, ShinyGO significant biological processes highlighted for all differentially expressed genes (FDR <0.05). **D** IPA enrichment analysis for all differentially expressed genes (FDR <0.05). EIF indicates eukaryotic initiation factor; FC, fold change; FDR, false discovery rate; GO, gene ontology; and IPA, ingenuity pathway analysis.

being downregulated (524; FDR <0.05; (Figure 3A and 3B). Transcriptomic analysis revealed significant downregulation of numerous oxidative phosphorylation components, including 15 genes encoding the cytochrome c oxidase enzyme complex: *Cox7c* (FDR, 3.5 E-38), *Cox5b*, (FDR, 8.1 E-22), *Cox17*, (FDR, 1.8 E-15), and *Cox6b1* (FDR, 3.6 E-10) and a series of 30 NADH dehydrogenase genes: *Ndufa3* (FDR, 1.1 E-36), *Ndufa1* (FDR, 1.3 E-26), *Ndufa2*, (FDR, 2.3 E-18), and *Ndufa5* (FDR, 6.0 E-16). Oxidative phosphorylation in the mitochondrion generates energy for the cell but also produces reactive oxygen species (ROS) as a by-product. Imbalance of ROS formation causes oxidative stress, which is a primary cause of embryopathy,[34] including diabetic embryopathy. To protect against ROS, the cell uses ROS scavenging enzymes. Interestingly, we observed significantly downregulated expression of 2 major ROS scavenging enzymes, *Sod1* (FDR, 3.8 E-5) and *Gpx4* (FDR, 0.02). These findings suggest a reduction in the cellular antioxidant capacity of developing hearts exposed to maternal obesity. Reduced antioxidant capacity, specifically due to downregulated *Sod1* and *Gpx4*, are similarly implicated in cardiac defects due to maternal diabetes.[23] Finally, in obesity-exposed hearts, RNA sequencing analysis displayed downregulation of several genes critical to cardiac development and maturation, including *Hand2* (FDR, 0.038) and a trend in *Myl2* (FDR, 0.073; P=0.0034).[35–39]

To further investigate the transcriptome profile of obesity exposed versus control embryonic day 12.5 embryonic hearts, with unbiased relation to biological processes, we used ShinyGO version 0.80 (Figure 3C, Table S2). The pathway analysis further highlighted a mechanism of oxidative phosphorylation and ROS imbalance, leading to oxidative stress, cell death, and cardiac damage. Top pathways included ribosome (fold enrichment, 28.34; FDR, 8.70 E-103), oxidative phosphorylation (fold enrichment, 20.02; FDR=3.96 E-61), diabetic cardiomyopathy (fold enrichment, 12.18; FDR, 2.23 E-42), chemical carcinogenesis–ROS (fold enrichment, 12.10; FDR, 4.11 E-46), and cardiac muscle contraction (fold enrichment, 8.67; FDR, 1.20 E-10)

(Figure 3C, Table S2). Additionally IPA for differentially expressed genes also indicated altered pathways, including oxidative phosphorylation (−log P=57.3), eukaryotic initiation factor (EIF) 2 signaling (−log P=53.8), mitochondrial dysfunction (−log P=37.3), granzyme A signaling (−log P=27.5), sirtuin signaling (−log P=27.5), Regulation of EIF4 and p70S6K signaling (−log P=16.1), mechanistic target of rapamycin (mTOR) signaling (−log P=13.3), necroptosis signaling pathway (−log P=4.69) and protein ubiquitination pathway (−log P=2.8) (Figure 3D, Table S3). Notably, disrupted sirtuin signaling further indicates reduced antioxidant capacity due to maternal obesity, given that sirtuin signaling, like *Sod1* and *Gpx4*, plays a primary role in ROS scavenging and the cell's antioxidant capacity to reduce oxidative stress.[40] Together, these data show clear activation of the cell's primary stress response, involving mTOR, EIF2, and EIF4 and resulting cell death, with activation of the granzyme pathway, necroptosis, and ubiquitination signaling. Of note, the top pathways impacted were oxidative phosphorylation and EIF2 signaling. EIF2 is the central hub of the cellular response to oxidative stress and drives global translation of proteins.[41] Therefore, we proceeded to analyze maternal obesity's impact on the global proteome of the developing embryonic heart.

Proteome Analysis Reveals Significant Translational Changes in Embryonic Hearts Exposed to Maternal Obesity

To investigate proteomic profile changes of maternal obesity–exposed day 12.5 embryonic hearts (n=4) versus control day 12.5 embryonic hearts (n=4), we used TMT-MS (Figure 4A.) Following global protein normalization and data filtering, a total of 7146 protein groups, 76 473 peptide groups, and 21 158 peptide-spectrum matches were identified. Initial TMT-MS data analysis revealed a total of 109 differentially expressed global proteins between maternal obesity and control embryonic hearts, specifically 40 upregulated (P<0.05) and 68 downregulated proteins (P<0.05) (Figure 4B and 4C). Further, to evaluate differential global protein expression between groups in relation to relative gene networks, we again used gene enrichment analysis using ShinyGO version 0.80 for biological processes. Similar to transcriptome studies, proteome analysis elucidated oxidative phosphorylation with ROS formation, oxidative stress, and cardiac damage, with significant processes of interest, including dilated cardiomyopathy (fold enrichment, 10.92; FDR, 4.03 E-03), arrhythmogenic right ventricular cardiomyopathy (fold enrichment, 10.70; FDR, 9.92 E-03), Hypertrophic cardiomyopathy (fold enrichment, 9.03, FDR=1.52 E-02), Oxidative phosphorylation (fold enrichment, 7.72; FDR=9.92 E-03), Cushing syndrome (fold enrichment, 6.34; FDR, 1.62 E-02), diabetic cardiomyopathy (fold enrichment, 6.04; FDR, 9.92 E-03), and chemical carcinogenesis–ROS (fold enrichment, 5.60; FDR, 1.20 E-02) (Figure 4D, Table S4). Similarly, IPA analysis revealed disrupted oxidative phosphorylation: mitochondrial dysfunction (−log P=3.84), oxidative phosphorylation (−log P=2.83); cellular stress response: regulation of EIF4 and p70S6K signaling (−log P=1.34); and cell death: necroptosis signaling pathway (−log P=1.5), granzyme B signaling (−log P=1.17), and ataxia telangiectasia mutated protein signaling (−log P=1.14) (Figure 4E, Table S5).

IPA global protein analysis interestingly revealed significant relation to several cell morphology and cytoskeleton arrangement pathways including: integrin-linked kinase signaling (−log P=1.92) and integrin signaling (−log P=1.17). Specifically, the pathway analysis implicated the actin cytoskeleton and cytoskeleton modifying Rho GTPase signaling pathway: actin cytoskeleton signaling (−log P=1.64), regulation of actin-based motility by Rho (−log P=2.77), Signaling by Rho family GTPases (−log P=2.92), actin nucleation by actin-related protein–Wiskott–Aldrich syndrome protein complex (−log P=2.09), RhoA signaling (−log P=1.76), Rac signaling (−log P=1.64), RhoGDI signaling (−log P=4.26), and Gαq signaling (−log P=1.4). Notably, the actin modifying Rho GTPase signaling pathway is critical to cardiac development.[42,43]

Phospho-Enriched Proteomic Analysis Reveals Significant Translational Changes in Embryonic Hearts Exposed to Maternal Obesity

Given the dysregulation of multiple kinases, including Rho kinases, in the global proteome analysis, we next performed phospho-enrichment followed by TMT-MS analysis (Figure 5). We identified 4647 phosophopeptides with 96% enrichment between high-fat and control–exposed embryonic day 12.5 embryonic hearts. Initial, TMT-MS data analysis revealed 62 differentially expressed (P<0.05) phosophoproteins, 52 of which were upregulated and 10 were downregulated (Figure 5A and 5B). IPA was used, again highlighting pathways relating to oxidative stress and the cytoskeleton. *Hif1* signaling was altered, (*Hif1*α signaling [−log P=1.9]), which is also involved in the balance of oxidative stress, and has been shown to contribute to the pathogenesis of cardiac defects due to diabetes.[23] Furthermore, IPA revealed a significant relation to cell stress and death, including mTOR signaling (−log P=3.85), 14–3-3 mediated signaling (−log P=2.49), regulation of EIF4 and p70S6K signaling (−log P=2.06), granulocyte-macrophage colony-stimulating factor signaling (−log P=1.94), chemokine signaling (−log P=1.81), EIF2 signaling (−log P=1.8), AMP-activated

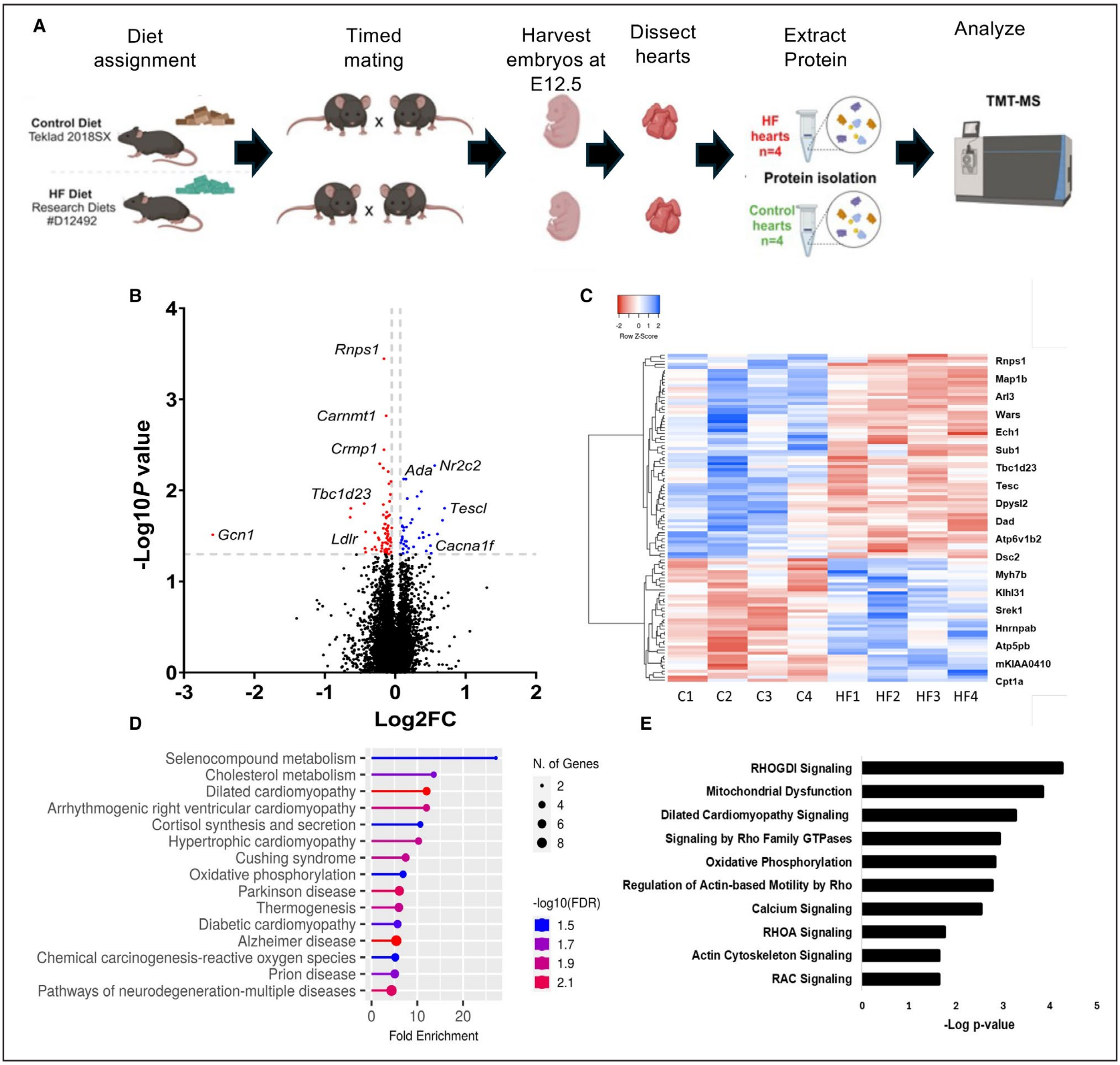

Figure 4. Global protein analysis of maternal obesity exposed and control embryonic hearts.
A, Schematic of diet exposure to establish obesity, followed by timed mating, embryo harvest at embryonic day 12.5, and heart dissection for TMT-MS, obesity exposed (n=4) versus control (n=4) embryonic day 12.5 wild-type embryonic hearts. **B**, One hundred nine significant differentially expressed global proteins observed between obesity-exposed versus control embryonic hearts (P<0.05). **C**, Heat map depicting significant differentially expressed global proteins (109) between obesity-exposed and control groups (P<0.05), with a random selection of 19 proteins displayed. **D**, ShinyGo significant biological pathways highlighted in enrichment analysis of all global proteins (P<0.05). **E**, IPA significant biological processes highlighted in enrigchment analysis of all global proteins (P<0.05). GO indicates gene ontology; HF, high-fat; IPA, ingenuity pathway analysis; and TMT-MS, tandem mass tag–mass spectroscopy.

protein kinase signaling (–log P=1.72), nerve growth factor signaling (–log P=1.49), cold shock domain containing E1 signaling pathway (–log P=2.12), and extracellular signal-regulated kinase 5 signaling (–log P=1.89) (Figure 5C, Table S6). Pathway analysis also indicated cytoskeleton signaling was altered, including integrin signaling (–log P=1.88) and integrin-linked kinase signaling (–log P=1.94). Rho GTPase signaling was again implicated, with altered RhoA signaling (–log P=1.47).

Pathway Enrichment Overlap

Integrating the transcriptomics and proteomics data demonstrates substantial areas of overlap, revealing insight into the mechanism for obesity-associated

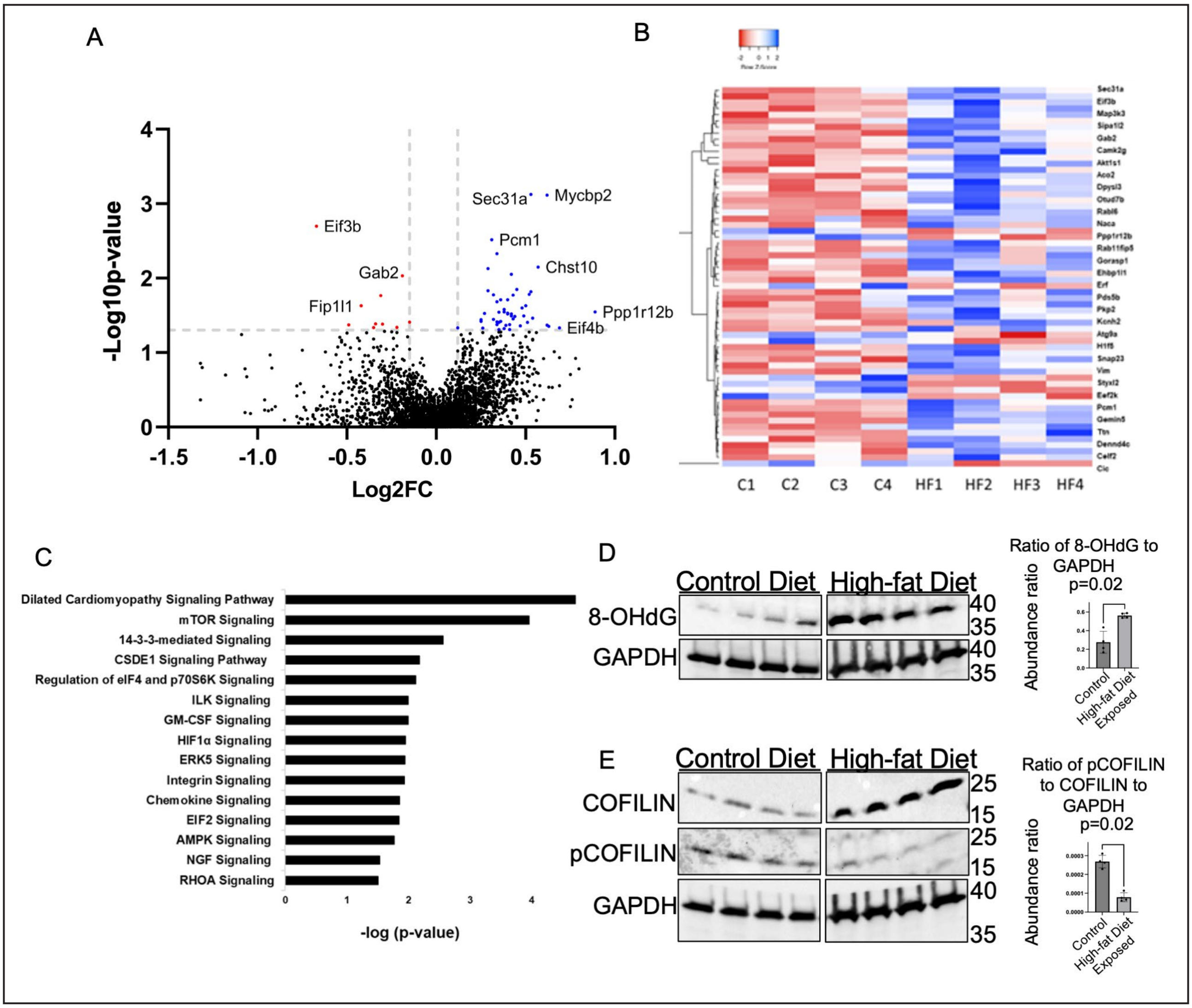

Figure 5. Phospho-proteomic analysis and immunoblot analysis of maternal obesity exposed and control embryonic hearts. Phospho-enriched TMT-MS from obesity-exposed (n=4) versus control (n=4) embryonic day 12.5 wild-type embryonic hearts. (**A**) Significant differentially expressed phosphoproteins (62) (*P*<0.05). **B**, Heat map depicting significant differentially expressed phosphoproteins (62) between obesity exposed and control groups (*P*<0.05), with a random selection of phosphoproteins displayed **C**, IPA significant biological processes highlighted for phosphoproteins (*P*<0.05). **D**, Immunoblot analysis of whole heart lysates from embryonic day 12.5 embryos, harvested from both high-fat diet–exposed and control dams, revealed a significant increase in the oxidative stress marker 8-OHdG in high-fat exposed embryonic hearts compared with controls (*P*=0.02 by Mann–Whitney test, with abundance ratio of 8-OHdG to GAPDH loading control, quantified in ImageJ). **E**, Additionally, there was an increase in the downstream Rho protein and Actin cytoskeletal regulator, cofilin, accompanied by a reduction in its activated, phosphorylated form in high-fat–exposed embryonic hearts compared with controls (*P*=0.02 by Mann–Whitney test, with abundance ratio of phosphorylated cofilin, to total cofilin, to GAPDH loading control, quantified in ImageJ). 8-OHdG indicates 8-hydroxy-2′-deoxyguanosine; FC, fold change; GO, gene ontology; HF, high-fat; IPA, ingenuity pathway analysis; and TMT-MS, tandem mass tag–mass spectroscopy.

CHD (Table S7). There were disease-related pathways, including cardiac disease pathways, with diabetic cardiomyopathy pathways, commonly enriched in both the transcriptome and proteome analysis of maternal obesity-exposed developing hearts (Table S7). In addition to diabetic cardiomyopathy, hypertrophic cardiomyopathy, and dilated cardiomyopathy were also top altered pathways in our proteome analysis.[44,45]

The overlapping pathways also reveal insight into mechanism. There is enrichment of a cascade of fundamental cellular processes implicated in embryopathy and birth defects, starting with oxidative phosphorylation and ROS formation, reduced antioxidant capacity, oxidative stress, cell death, and cytoskeletal signaling disruption. These mechanisms are implicated in infant birth defects including the heart defects associated with maternal diabetes.[23] Every pathway analysis, including both the altered transcriptome and proteome data sets, demonstrated enrichment of oxidative phosphorylation (Table S7). In the cell, oxidative phosphorylation generates ROS, and sirtuin signaling has a pivotal role in cellular handling of antioxidant function and ROS balance.[40] Sirtuin signaling was also significantly altered in both transcriptome and proteome analysis due to maternal obesity (Table S7). Evidence of ROS burden was present, with chemical carcinogenesis–ROS indicated in transcriptome and proteome analyses (Table S7). There was also evidence of resulting oxidative stress, with key markers of the cellular stress response enriched, including mTOR, EIF2, and EIF4-related signaling pathways (Table S7). EIF2 signaling is the central hub of the cell's integrated stress response, and EIF2 signaling was a top pathway altered in both the transcriptome and proteome. There was evidence of cell death pathways, including granzyme signaling and necroptosis signaling, commonly altered in both the transcriptome and proteome (Table S7).

To investigate oxidative stress in developing hearts, we performed immunoblot assays for the well-established oxidative stress biomarker, 8-OHdG, which is a product of oxidative damage to nuclear and mitochondrial DNA and has been used to quantify oxidative damage in humans due factors ranging from tobacco smoke to heavy metals, and its presence has been linked to birth defects.[46,47] Our analysis revealed significantly increased levels of 8-OHdG in the high-fat–exposed embryo hearts (Figure 5D, Figure S2).

Finally, both the global protein and phosphoprotein analysis revealed numerous altered pathways that are related to the actin cytoskeleton including numerous factors related to the actin cytoskeleton–modifying Rho GTPase signaling pathway, which is critical to cardiac development[42,43] and oxidative stress is known to impact Rho GTPase signaling in the heart.[48] Rho GTPase signaling is a key regulator of semaphorin signaling, and semaphorin signaling is also critical for cardiac development and neural crest cell migration.[49,50] Semaphorin signaling emerged as a top pathway in the global proteome analysis, ranking first and eighth among the most significantly altered pathways by −log *P* value (Table S5). It was also prominently featured in the phosphoproteome analysis, ranking as the sixth most significantly altered pathway by −log *P*-value (Table S6). Rho GTPase and semaphorin signaling regulate the phosphorylation of cofilin, a key regulator of the actin cytoskeleton in the cell.[51] In cardiomyocytes, oxidative stress causes aggregation of cofilin and loss of cofilin phosphorylation.[52] We assessed cofilin phosphorylation in the developing heart by immunoblot analysis. Immunoblotting for total and phosphorylated cofilin revealed a visible increase in total cofilin, possibly indicating upregulation or aggregation under oxidative stress conditions. Conversely, phosphorylated cofilin was notably decreased in obesity-exposed embryos. The ratio of phosphorylated to total cofilin was significantly decreased in obesity-exposed embryos (Figure 5E, Figure S2), confirming disruption to actin cytoskeleton related pathways.

Previous studies have demonstrated that there is generally little overlap between transcriptomic and proteomic data sets at the gene/protein level, due to differences in the half-lives of mRNA and proteins, posttranscriptional modifications, and posttranslational modifications, in addition to biases in data collection and statistical methodology inherent to the technologies.[53] However, we identified 5 overlapping genes/proteins. We performed pathway analysis of the 5 overlapping genes/proteins, which again highlighted oxidative phosphorylation as the top Kyoto Encyclopedia of Genes and Genomes pathway impacted (P=0.033), and the ShinyGO analysis similarly identified oxidative phosphorylation and other interesting pathways related to cardiac pathology, including dilated cardiomyopathy (Table S7).

Maternal Obesity Exposure During Development Causes Cardiac Defects in Mice

Both the global proteome and phosphoproteome analysis indicated disruption to the actin cytoskeleton and to the actin-modifying Rho GTPase signaling pathway. We recently identified a novel CHD candidate gene called *Shroom3*, which is required for the function of Rho kinase signaling. SHROOM3 binds actin, Rho associated kinase 1 and 2.[54–59] SHROOM3 loss-of-function implicated neural tube defects are influenced by gene–environment interaction, including maternal folic acid diet[60] and maternal diabetes.[61] SHROOM3 loss-of-function CHDs[62] phenocopy CHDs implicated in maternal obesity. Therefore, we hypothesized the partially penetrant cardiac defects due to SHROOM3 loss-of-function would be modifiable with obesity. To test this hypothesis, we placed *Shroom3*$^{+/gt}$ females on a high-fat diet or control diet from weeks 5 onward (Figure S3). We confirmed diet-induced obesity model establishment in *Shroom3*^{gt} dams by body composition analysis via EchoMRI at week 5 for baseline readings and then again at week 9, along with a glucose check, for assessment of obesity establishment in the respective diet cohorts. We again observed a significant change in weight and body fat, without a significant change in glucose. Notably, there was a more pronounced change in weight and body fat and significantly decreased lean body mass in the obesity-exposed dams compared with the controls, which differed from wild-type dams (Figure S3). We then set the females up in timed mating with *Shroom3*$^{+/gt}$

males. This yielded litters of SHROOM3 null embryos, *Shroom3*$^{gt/gt}$ (25%), in addition to heterozygous littermates, *Shroom3*$^{+/gt}$ (50%), and wild-type littermate controls, *Shroom3*$^{+/+}$ (25%). There were trends related to pregnancy, where obese females were less likely to get pregnant than controls (frequency, 0.57 versus 0.83) and obese females had slightly smaller litters than controls (litter size, 6.4 versus 7.5), as demonstrated in previous studies.[26] We analyzed 109 embryos, and there was no impact on embryo survival, with no statistically significant differences in the distribution of embryo genotypes between diet cohorts (Figure 6D). However, there was a significant increase in the frequency of cardiac defects after obesity exposure. Across the entire cohort, compared with controls, the frequency of membranous ventricular septal defects (VSDs) more than doubled in the high-fat diet–exposed embryos (frequency, 0.1 versus 0.26; P=0.04). Within genotypes, the trend persisted, where compared with controls, the obesity-exposed embryos had a higher frequency of VSDs in every genotype analyzed, with a significant increase in wild-type littermates (0 versus 0.27, P=0.01), and a trend of increased VSDs, doubling in *Shroom3*$^{gt/gt}$ embryos (frequency, 0.2 versus 0.42) and increasing in *Shroom3*$^{+/gt}$ embryos (0.1 versus 0.13; Figure 6E). The data within the *Shroom3* embryo groups was not statistically significant, and revealed only an additive number of cardiac defects. However, overall, the data show that obesity-exposed embryos exhibit a significant increase in the frequency of embryonic membranous VSDs.

Collectively, all of the data presented indicate that maternal obesity exposure disrupts embryonic cardiac development.

DISCUSSION

Using a clinically relevant diet-induced maternal obesity murine model, we observed significant transcriptome, proteome, and cellular changes, with resulting cardiac defects, in developing embryonic hearts, due to maternal obesity. These data offer insight into the poorly understood molecular mechanisms and developmental programming involved in embryonic cardiogenesis, which is disrupted under maternal obesity.

In our study, we used a murine model of maternal obesity, which attempts to mirror the conditions of obesity seen in human patients. While models used to investigate maternal diabetes and obesity have often used genetic modifications, streptozocin injection to destroy pancreatic cells, or high-carbohydrate diets, with resulting extreme elevations in blood glucose,[63] our model strictly uses a high-fat diet to induce maternal obesity. The high-fat diet–induced maternal obesity model is well established, and is increasingly being used to generate obesity without diabetes.[32] The model has been shown to avoid gestational diabetes, with normal blood glucose persisting through gestation, up to embryonic day 17, where physiologic insulin resistance peaks during pregnancy[32]; therefore, in our study, we avoided glucose rechecks between mating and our analyses at embryonic days 12.5 and 14.5, given that they have been shown to induce inflammation and spontaneous abortions,[64] which would impact our findings. In our study, we observed some expected variable penetrance of the obesity phenotype due to pleiotropy.[65] However, overall, there was a significant increase in body weight and body fat composition with no significant difference in glucose levels. There was a slight difference in GTT and ITT, at certain time points, likely indicating a state of developing insulin resistance, despite normal fasting and fed blood glucose levels (Figure 1, Figure S1). Overall, the model accurately reflects the condition of obesity seen in human patients.

Previous studies demonstrate that after exposure to diet-induced maternal obesity, offspring have no difference in body weight or body composition, even in pups up to 8 weeks of age; however, maternal obesity resulted in changes to the offspring's heart, including increased offspring cardiac mass and evidence of hyperinflammation in the postnatal myocardium.[66] In our study, we extended these findings to the embryonic heart and showed an impact on cardiac development. We demonstrate that despite normal blood glucose, obesity-exposed embryos display cardiac defects similar to those attributed to maternal hyperglycemia. This indicates maternal obesity, due to either lipotoxicity or possibly an inappreciable level of hyperglycemia, may be sufficient to disrupt cardiac development and lead to cardiac defects.

Pathway analysis of the altered transcriptome and proteome revealed mechanistic insight into the cardiac defects related to maternal obesity. There was substantial overlap in cardiac disease–related signaling pathways, including diabetic cardiomyopathy, which was significantly enriched in both transcriptome and proteome analyses, as well as hypertrophic and dilated cardiomyopathy. Oxidative phosphorylation was significantly altered in every pathway analysis performed from both transcriptome and proteome studies of developing hearts. Oxidative phosphorylation is the final step in ATP generation by the mitochondrion, and also generates ROS that causes cellular damage due to oxidative stress. Disruption to oxidative phosphorylation itself causes cardiac dysfunction,[67,68] and oxidative stress from ROS is a primary cause of chemical carcinogenesis and embryopathies, including cardiac defects.[69] Indeed, the pathway "chemical carcinogenesis ROS" was a top gene ontology pathway in both the transcriptome and proteome analysis of affected genes and proteins due to maternal obesity. Prior

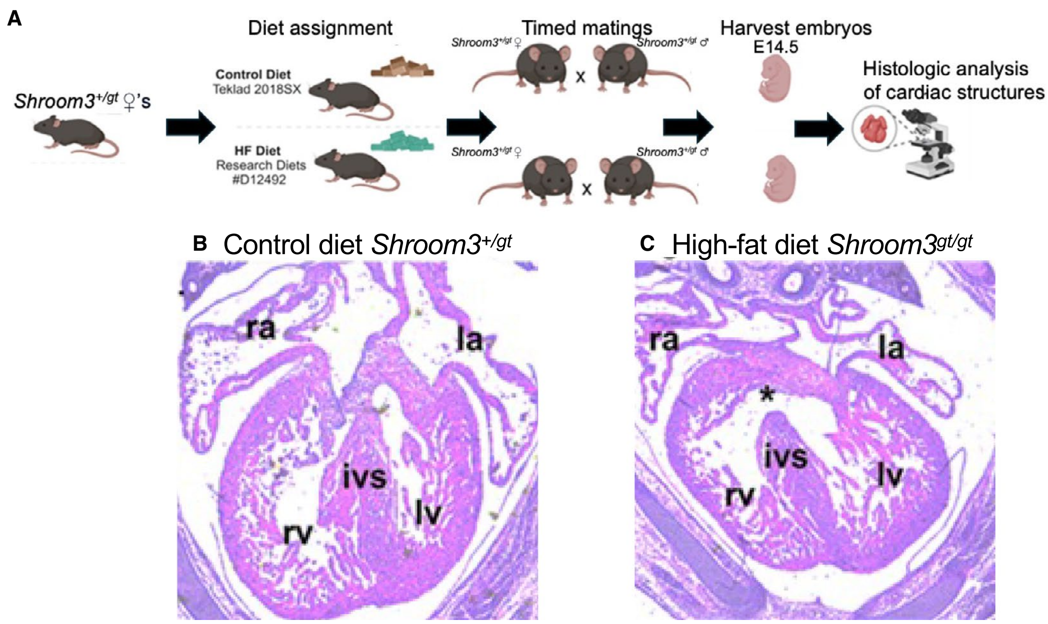

	Control Diet		High-Fat Diet	
D	Number of embryos	Frequency of genotype	Number of embryos	Frequency of genotype
Shroom3$^{+/+}$	19	0.23, *P*=0.72	11	0.29, *P*=0.78
Shroom3$^{+/gt}$	48	0.58, *P*=0.28	15	0.39, *P*=0.36
Shroom3$^{gt/gt}$	16	0.19, *P*=0.72	12	0.32, *P*=0.61
Total	83		38	
E	Embryos with membranous VSD	Frequency of VSD within genotype	Embryos with membranous VSD	Frequency of VSD within genotype
Shroom3$^{+/+}$	0 of 19	0.00	3 of 11	0.27, *P*=0.016
Shroom3$^{+/gt}$	5 of 48	0.10	2 of 15	0.13, *P*=0.75
Shroom3$^{gt/gt}$	3 of 16	0.20	5 of 12	0.42, *P*=0.18
Total	8 of 83	0.096	10 of 38	0.26, *P*=0.016

Figure 6. Assesment of maternal obesity-exposed and control embryos for cardiac defects.
A, *Shroom3*^{gt} female mice were placed on a high-fat diet or control diet from 5 weeks of life to 9 weeks of life to generate obesity. Obese and control *Shroom3*$^{+/gt}$ females were then placed in timed mating with *Shroom3*$^{+/gt}$ males. Embryos were harvested at embryonic day 14.5 and hematoxylin and eosin–stained sections of the entire heart were reviewed. **B**, The membranous ventricular septum generally closes at embryonic day 14.5, here in a *Shroom3*$^{+/gt}$ embryo, from a control dam. **C**, A membranous VSD occurs where the ventricular septum fails to close, here in a *Shroom3*$^{gt/gt}$ embryo from an obese dam (asterisk). (**D**) Analysis of 121 embryos revealed no significant difference in embryo genotypes between control and high-fat diet exposed embryos (by χ^2 analysis of the observed to expected genotype ratios.) **E**, In wild-type littermates, there were significantly increased VSDs (0 versus 0.27, *P*=0.016), and a trend of increased VSDs, in *Shroom3*$^{gt/gt}$ embryos, (frequency, 0.2 versus 0.42) and in *Shroom3*$^{+/gt}$ embryos (0.1 versus 0.13). Across the entire cohort, the frequency significantly increased (0.096 versus 0.26, *P*=0.016) (by χ^2 analysis of septal defects, comparing control with maternal obesity–exposed embryos within each genotype and within the whole cohort.) *Ventricular septal defect. HF indicates high-fat; gt, gene trap; ivs, intraventricular septum; la, left atrium; lv, left ventricle; ra, right atrium; rv, right ventricle; and VSD, ventricular septal defect.

studies have demonstrated maternal obesity results in altered oxidative phosphorylation and oxidative stress,[70,71] and our data indicate that these processes alter the transcriptome, proteome, and morphology of the developing heart.

The developing embryo balances oxidative stress due to ROS with antioxidant factors, including ROS scavenging enzymes, comprising *Sod1* and *Gpx4*,[23] activation of the sirtuin signaling pathway,[40] and inducing the *Hif1* pathway. Exposure to maternal teratogens, including that of maternal diabetes, reduces the antioxidant capacity in embryos and in the heart, this mechanism has been implicated in cardiac defects, including VSDs and persistent truncus arteriosus.[72] In obesity-exposed embryo hearts, we noted a similar significant reduction in the antioxidant capacity of developing embryo hearts. Transcriptome profiling displayed significant dysregulation of *Sod1* and *Gpx4*. Sirtuin signaling was impacted in both the transcriptome and proteome pathway analysis. The phosphoproteome also indicated significant disruption to *Hif1a* signaling in the maternal obesity–exposed embryonic day 12.5 embryo hearts. *Sod1* and *Gpx4* are also specifically implicated in cardiac defects due to maternal diabetes,[23] with *Sod1* and *Gpx4* activity being decreased in malformed embryos of Sprague–Dawley rats.[73,74] Overexpression of *Sod1* rescues maternal diabetes-induced cardiac phenotypes, including VSDs, by mitigating activity of oxidative stress markers in developing cardiac structures.[72,75,76] Maternal diabetes also inhibits *Hif1a*, and this mechanism is implicated as a primary mechanism leading to the cardiac defects in maternal diabetes.[23] Together, these data suggest that disrupted cardiogenesis due to maternal obesity likely results from aberrant processes of ROS homeostasis and antioxidant capacity, enabling embryonic susceptibility to oxidative stress, with subsequent teratogenic effects in the developing heart.

Our data suggest oxidative stress as a primary molecular teratogen in maternal obesity exposure, and IPA analysis revealed stress-related pathways, including EIF2 and EIF4, impacted in both the transcriptome and proteome. Of note, EIF2 was a top pathway impacted and serves as the regulatory hub of the cell's integrated stress response,[77] driving protein translation response, and EIF2 is specifically implicated as a mediator in cardiac and vascular cardioprotective homeostasis.[78,79] Previous literature has also shown that inhibition of the sirtuin pathway exacerbates endoplasmic reticulum stress-induced apoptosis in cardiomyocytes, directly triggering EIF2 pathway hyperactivation.[80] In human and animal models, maternal obesity exposure is associated with oxidative stress, leading to increased expression of endoplasmic stress markers in placental tissue[68,81–83] and caspase-dependent apoptosis activity in developing cardiac structures.[73] Conversely, exposure to maternal obesogenic feeding decreases placental EIF2α phosphorylation in rats and triggers increased expression in proapoptotic markers.[84–86] We demonstrated that embryo hearts exposed to maternal obesity had elevated levels of 8-OHdG, which is a by-product of oxidative damage to nuclear and mitochondrial DNA and is commonly used as a biomarker to quantify oxidative stress caused by environmental teratogens and has been linked to birth defects.[46,47] Overall, these data support a mechanism of obesity-related cardiac defects resulting from oxidative stress and promoting teratogenic effects in the embryo.

The transcriptome and proteome analysis of embryonic hearts exposed to maternal obesity had numerous disrupted pathways related to the actin cytoskeleton, with several pathways directly related to the modulation of actin by Rho GTPase signaling. The Rho GTPase signaling pathway is critical for cardiac development,[42,43] and oxidative stress is known to impact this pathway in the heart.[48] Rho GTPase signaling is a key regulator of semaphorin signaling, which is also essential for cardiac development, driving neural crest cell migration to the outflow tract and ventricular septum.[49,50] Semaphorin signaling emerged as the top pathway altered in the global proteome analysis and was also implicated in the phosphoproteome analysis. Rho GTPase and semaphorin signaling regulate the phosphorylation of cofilin, a key regulator of the actin cytoskeleton.[51] Oxidative stress causes cofilin aggregation and a loss of cofilin phosphorylation,[52] and we demonstrated a decrease in activated, phosphorylated cofilin in obesity-exposed embryonic hearts (Figure 5D).

In RhoGTPase signaling, cofilin is directly downstream of Rho-associated coiled-coil–containing protein kinases (ROCKs).[42] ROCKs consist of 2 isoforms, ROCK1 and ROCK2, which act as major downstream effectors of Rho GTPase and play a central role in actin cytoarchitecture.[42,87] ROCK1 and ROCK2 are known to play a role in cardiac cell physiology[88,89] and cardiac development, with deletion in either cardiac or neural crest lineages leading to embryonic lethality.[42,43] ROCK1 and ROCK2 are downstream effectors of noncanonical WNT/planar cell polarity (WNT/PCP) signaling,[90] a fundamental pathway that drives cell polarization, shape, and movement, and WNT/PCP dysregulation causes CHD.[91–101] Multiple prior studies show that obesity impacts WNT/PCP signaling,[102–105] and further studies are needed to explore whether obesity-related cardiac defects are due, in part, to WNT/PCP dysregulation.

In parallel to oxidative stress and Rho GTPase signaling, our data highlighted several pathways related to cell death, including the activation of the granzyme pathway, necroptosis, and ubiquitination signaling. Previous studies demonstrate that ROCK1 and ROCK2 play a vital role in the regulation of cell death processes,[106,107] mediating cell survival,[108] and apoptosis-mediated cell death,[109,110] via actin cytoskeleton regulation. In particular, after exposure to oxidative stress, Rho kinase signaling and ROCK1/2 play a fundamental role in cell survival by modulating actin stability.[111] However, other studies have noted that Rho GTPase signaling mediates a positive feedback loop of ROS generation, where ROS activate Rho kinase signaling, exacerbating oxidative stress.[112] Further insight is required to elucidate how these pathways may concomitantly interact to induce cardiac anomalies in offspring.

The function of ROCK1 and ROCK2 are dependent on a protein called SHROOM3, which binds ROCK1/2 and F-ACTIN, recruits them to the cell membrane, and facilitates activation of their kinase domian.[55] SHROOM3 is implicated in patients with CHD[113–115] and has a role in the heart after myocardial infarction.[115] We recently showed that *Shroom3$^{gt/gt}$* mice display cardiac defects, and we implicated dysregulated WNT/PCP signaling.[62] Interestingly, gene–environment interaction play an important role in *Shroom3* loss-of-function implicated neural tube defects, being modulated by folic acid[60] and impacted by maternal diabetes.[61] Here, we tested the hypothesis that maternal obesity would similarly increase the penetrance of cardiac defects due to *Shroom3* loss of function. The diet-induced obesity model was successful in the *Shroom3^{gt}* dams, and notably, the impact seemed to be more pronounced, with a greater increase in weight and body fat, and a significantly decreased lean body mass. However, while there was a trend of increased membranous VSDs in the obesity-exposed embryos, compared with controls, more than doubling in *Shroom3$^{gt/gt}$* embryos, the differences were not statistically significant in the SHROOM3 groups. Furthermore the additional VSDs appeared to be additive in the SHROOM3 group, suggesting that SHROOM3 and maternal obesity may not interact. However, the sensitized genetic background of the *Shroom3$^{+/gt}$* dam heightened the maternal response to the high-fat diet, as indicated, and this may have impacted cardiac development, even the wild-type embryos in the litter that did reach statistical significance. Future studies should involve more in-depth and mechanistic exploration at the interface of SHROOM3, ROCK1/2, Rho GTPase, the actin cytoskeleton, WNT/PCP, oxidative stress, and cell death during heart development. In the current study, involving analysis of >100 embryos, the most substantial finding was a doubling of cardiac defects in every genotype, including a significant increase in the penetrance of cardiac defects in the wild-type embryos exposed to maternal obesity.

In our analysis of embryonic cardiac defects, we demonstrated that obese females were less likely to get pregnant than controls and obese females had slightly smaller litters compared with controls, similar to previous studies. However, most importantly, in embryos, there was significantly increased penetrance of membranous VSDs in obesity-exposed embryos (Figure 6). This shows that the altered developmental programs, indicated by the transcriptome and proteome analysis, disrupts cardiac development sufficiently to result in embryonic cardiac defects. Previous studies in murine models of maternal obesity have demonstrated programming impacting the heart, including offspring cardiac hypertrophy[66] and dysfunction,[116,117] and have also provided mechanistic insight.[70,71] Our data support these studies and build upon their findings using single-cell and multiomics analysis, demonstrating overlapping mechanisms, including oxidative stress. Offspring cardiac septal defects have been identified in murine models of maternal diabetes. However, this study is the first, to our knowledge, to use a murine model of maternal obesity to identify offspring septal defects. The findings reflect the septal defects associated with maternal obesity in human patients and begin to shed light on their pathogenesis.

The snRNAseq data were limited by small sample size. Despite this limitation, quantifying the total number of cells in each cluster provided valuable insight into cardiomyocyte differences between control and high-fat diet embryos. They demonstrated a shift in the cardiomyocyte population with a decrease in the number of mature cardiomyocytes and an increase in immature cardiomyocytes in the obesity-exposed embryos. Oxidative stress significantly impacts cardiomyocyte maturation, with DNA damage from oxidative stress affecting cardiomyocyte proliferation and differentiation potential.[118] Confirmatory transcriptomic analysis with bulk RNA sequencing supports this mechanism with downregulation of the cardiomyocyte maturation marker *Myl2* as well as *Hand2*. *Hand2* is a basic helix–loop family transcription factor, which is ubiquitously expressed within second heart field cardiac progenitor cells to aid outflow tract and cardiac looping formation.[119,120] Previous systemic *Hand2* knockout models display embryonic lethality due to cardiac malformation. Recently, single-cell transcriptomic profiling revealed that maternal diabetes exposure impedes second heart field–derived cardiomyocyte differentiation, which was attributed to impaired and downregulated function of cell lineage specifying transcription factors, including *Hand2*.[24] WNT/PCP is required in the second heart field during cardiac development.[121] Studies have also demonstrated that antioxidant capacity and ROS scavenging machinery are reduced in the right ventricle and second heart field.[122] Collectively, these findings could also suggest that maternal obesity disrupts the second heart field, through oxidative stress, WNT/PCP dysregulation, or both, and future studies should explore this mechanism further, possibly using expanded snRNAseq, multiomics analysis, and spatial transcriptomics.

Obesity is a modifiable environmental risk factor that can be addressed through lifestyle changes, surgical interventions, and pharmaceuticals, with recent advances in glucagon-like peptide 1 agonists and sodium–glucose cotransporter 2 inhibitors increasing promise.[123] Furthermore, one of the primary findings in our study is increased oxidative stress associated with cardiac defects, suggesting that antioxidant therapy may be a useful to reduce maternal obesity–induced CHD. Antioxidant therapy has been used to reduce oxidative stress due to diabetes.[124] However, a recent report demonstrated that a sensitized genetic background impacted the response of embryos to antioxidant therapy, mitigating the effect in reducing the cardiac defects due to maternal diabetes.[125] These important findings indicate that further analysis of gene–environment interactions is needed to help understand pathophysiology and help guide therapy for CHD, the most common birth defect.

In conclusion, these data demonstrate that maternal obesity exposure disrupts the transcriptome, proteome, and phosphoproteome in the developing heart. Specifically, our data revealed disrupted expression of genes related to oxidative phosphorylation, reduced antioxidant capacity, oxidative stress, Rho GTPase signaling, and cytoskeletal signaling disruption in developing hearts. We also show cardiac defects in a murine model. These findings begin to assess the underlying complex pathology of maternal obesity exposure and direct impact on cardiac development. Further research is required to fully understand causal molecular mechanisms, and guide therapy, as maternal obesity rates continue to increase among the global population along with the conferred risk of CHD in offspring.

ARTICLE INFORMATION

Received October 24, 2024; accepted March 21, 2025.

Affiliations

Department of Pediatrics, Herman B Wells Center for Pediatric Research, Indiana University School of Medicine, Indianapolis, IN (A.M., N.J., L.S.H., W.S., K.L.K., S.K.H., M.D.D.); Department of Biology, Stanford University, Stanford, CA (J.B.Z.); and Center for Diabetes and Metabolic Disease Research, Indiana University School of Medicine, Indianapolis, IN (K.L.K.).

Acknowledgments

The authors thank the Center for Diabetes and Metabolic Diseases Islet and Physiology Core (P30DK097512), Center for Proteome Analysis, Center for Medical Genomics, and Bioinformatics Core at the Indiana University School of Medicine for their assistance in this project. The Center for Medical Genomics at Indiana University School of Medicine is partially supported by the Indiana University Grand Challenges Precision Health Initiative. The mass spectrometry work was performed by the Indiana University School of Medicine Center for Proteome Analysis, Emma H. Doud and Whitney Smith-Kinnaman. Acquisition of the Indiana University School of Medicine Center for Proteome Analysis instrumentation used for this project was provided in part by the Indiana University Precision Health Initiative and the Indiana University Simon Comprehensive Cancer Center. The proteomics work was supported, in part, by the Indiana Clinical and Translational Sciences Institute (Award Number UL1TR002529 from the National Institutes of Health, National Center for Advancing Translational Sciences, Clinical and Translational Sciences Award), and the P30 Indiana University Simon Comprehensive Cancer Center Support Grant, (Award Number P30CA082709 from the National Cancer Institute). During the preparation of this work, the authors used Grammarly and Microsoft Copilot to check grammar and spelling and improve readability. After using this tool, the authors reviewed and edited the content as needed and take full responsibility for the content of the published article.

Author contributions: Conceptualization: M.D.D. and L.H.; methodology: A.M., J.Z., K.L.K., and S.K.H.; software: S.K.H.; validation: M.D., K.L.K., and S.K.H.; formal analysis: J.Z., A.M., and S.K.H.; resources: M.D.; data curation: A.M., J.Z., and SH; writing—original draft preparation: A.M.; writing—review and editing: AM., J.Z., L.H., W.S., K.L.K., S.K.H., and M.D.D.; supervision, M.D.D.; project administration: M.D.D.; funding acquisition: M.D.D. All authors have read and agreed to the published version of the manuscript.

Sources of Funding

This study was supported by a National Institutes of Health (Bethesda, MD) 5K08HL148508 Award (M.D.D.), P01HL345599 (M.D.D. and W.S.) Award, 5K08 HD109636 (K.L.K.), the American Heart Association Career Development Award 861 914 (S.K.H.), March of Dimes Basil O'Connor Award (K.L.K.), the Riley Children's Foundation and the Herman B. Wells Center for Pediatric Research at Indiana University School of Medicine.

Disclosures

None.

Supplemental Material

Tables S1–S7
Figures S1–S3

REFERENCES

1. Boneva RS, Botto LD, Moore CA, Yang Q, Correa A, Erickson JD. Mortality associated with congenital heart defects in the United States: trends and racial disparities, 1979–1997. *Circulation*. 2001;103:2376–2381. doi: 10.1161/01.cir.103.19.2376
2. Lopes SAVA, Guimarães ICB, Costa SFO, Acosta AX, Sandes KA, Mendes CMC. Mortality for critical congenital heart diseases and associated risk factors in newborns. A cohort study. *Arquivos Brasileiros Cardiologia*. 2018;111:666–673. doi: 10.5935/abc.20180175
3. Reller MD, Strickland MJ, Riehle-Colarusso T, Mahle WT, Correa A. Prevalence of congenital heart defects in metropolitan Atlanta, 1998-2005. *J Pediatr*. 2008;153:807–813. doi: 10.1016/j.jpeds.2008.05.059
4. Oster ME, Lee KA, Honein MA, Riehle-Colarusso T, Shin M, Correa A. Temporal trends in survival among infants with critical congenital heart defects. *Pediatrics*. 2013;131:e1502–e1508. doi: 10.1542/peds.2012-3435
5. Van Der Linde D, Konings EE, Slager MA, Witsenburg M, Helbing WA, Takkenberg JJ, Roos-Hesselink JW. Birth prevalence of congenital heart disease worldwide: a systematic review and meta-analysis. *J Am Coll Cardiol*. 2011;58:2241–2247. doi: 10.1016/j.jacc.2011.08.025
6. Fahed AC, Gelb BD, Seidman J, Seidman CE. Genetics of congenital heart disease: the glass half empty. *Circul Res*. 2013;112:707–720.
7. Russell MW, Chung WK, Kaltman JR, Miller TA. Advances in the understanding of the genetic determinants of congenital heart disease and their impact on clinical outcomes. *J Am Heart Assoc*. 2018;7:e006906. doi: 10.1161/JAHA.117.006906
8. Kalisch-Smith JI, Ved N, Sparrow DB. Environmental risk factors for congenital heart disease. *Cold Spring Harbor Pers Biol*. 2020;12:a037234. doi: 10.1101/cshperspect.a037234
9. Feng Y, Yu D, Yang L, Da M, Wang Z, Lin Y, Ni B, Wang S, Mo X. Maternal lifestyle factors in pregnancy and congenital heart defects in offspring: review of the current evidence. *Italian J Pediatr*. 2014;40:1–7.
10. Zhu Y, Chen Y, Feng Y, Yu D, Mo X. Association between maternal body mass index and congenital heart defects in infants: a meta-analysis. *Congenital Heart Dis*. 2018;13:271–281. doi: 10.1111/chd.12567
11. Mills JL, Troendle J, Conley MR, Carter T, Druschel CM. Maternal obesity and congenital heart defects: a population-based study. *Am J Clini Nutr*. 2010;91:1543–1549. doi: 10.3945/ajcn.2009.28865
12. Liu X, Ding G, Yang W, Feng X, Li Y, Liu H, Zhang Q, Ji L, Li D. Maternal body mass index and risk of congenital heart defects in infants: a dose-response meta-analysis. *Biomed Res Int*. 2019;2019:1–14. doi: 10.1155/2019/1315796
13. Persson M, Cnattingius S, Villamor E, Söderling J, Pasternak B, Stephansson O, Neovius M. Risk of major congenital malformations in relation to maternal overweight and obesity severity: cohort study of 1.2 million singletons. *Bmj*. 2017;357:j2563. doi: 10.1136/bmj.j2563
14. Rosenbluh O, Walfisch A. Birth defects associated with obesity. 2021.

15. Collaborators G, Ärnlöv J. Global burden of 87 risk factors in 204 countries and territories, 1990–2019: a systematic analysis for the global burden of disease study 2019. *Lancet*. 2020;396:1223–1249.
16. Turunen R, Pulakka A, Metsälä J, Vahlberg T, Ojala T, Gissler M, Kajantie E, Helle E. Maternal diabetes and overweight and congenital heart defects in offspring. *JAMA Netw Open*. 2024;7:e2350579. doi: 10.1001/jamanetworkopen.2023.50579
17. Brite J, Laughon SK, Troendle J, Mills J. Maternal overweight and obesity and risk of congenital heart defects in offspring. *Intern J Obesity*. 2014;38:878–882.
18. Persson M, Razaz N, Edstedt Bonamy A-K, Villamor E, Cnattingius S. Maternal overweight and obesity and risk of congenital heart defects. *J Am Coll Cardiol*. 2019;73:44–53. doi: 10.1016/j.jacc.2018.10.050
19. Madsen NL, Schwartz SM, Lewin MB, Mueller BA. Prepregnancy body mass index and congenital heart defects among offspring: a population-based study. *Congenital Heart Dis*. 2013;8:131–141. doi: 10.1111/j.1747-0803.2012.00714.x
20. Nishino T, Ranade SS, Pelonero A, van Soldt BJ, Ye L, Alexanian M, Koback F, Huang Y, Wallace LG, Sadagopan N. Single-cell multimodal analyses reveal epigenomic and transcriptomic basis for birth defects in maternal diabetes. *Nat Cardiovasc Res*. 2023;2:1190–1203.
21. Basu M, Zhu J-Y, LaHaye S, Majumdar U, Jiao K, Han Z, Garg V. Epigenetic mechanisms underlying maternal diabetes-associated risk of congenital heart disease. *JCI Insight*. 2017;2:2. doi: 10.1172/jci.insight.95085
22. Steimle JD, Martin JF. Sweet and sour story of maternal diabetes and birth defects. *Nature Cardiovasc Res*. 2023;2:1107–1108. doi: 10.1038/s44161-023-00380-1
23. Basu M, Garg V. Maternal hyperglycemia and fetal cardiac development: clinical impact and underlying mechanisms. *Birth Defects Res*. 2018;110:1504–1516. doi: 10.1002/bdr2.1435
24. Manivannan S, Mansfield C, Zhang X, Kodigepalli KM, Majumdar U, Garg V, Basu M. Single-cell transcriptomic profiling unveils dysregulation of cardiac progenitor cells and cardiomyocytes in a mouse model of maternal hyperglycemia. *Commun Biol*. 2022;5:820. doi: 10.1038/s42003-022-03779-x
25. Basu M, Bosse K, Garg V. Notch1 haploinsufficiency increases risk of congenital heart defects in the setting of maternal diabetes by an epigenetic mechanism. *Circulation*. 2014;130:A19285.
26. Gao X, Li Y, Ma Z, Jing J, Zhang Z, Liu Y, Ding Z. Obesity induces morphological and functional changes in female reproductive system through increases in NF-κB and MAPK signaling in mice. *Reprod Biol Endocrinol*. 2021;19:1–15. doi: 10.1186/s12958-021-00833-x
27. du Percie Sert N, Hurst V, Ahluwalia A, Alam S, Avey MT, Baker M, Browne WJ, Clark A, Cuthill IC, Dirnagl U. The ARRIVE guidelines 2.0: updated guidelines for reporting animal research. *J Cereb Blood Flow Metab*. 2020;40:1769–1777.
28. Grecco GG, Haggerty DL, Doud EH, Fritz BM, Yin F, Hoffman H, Mosley AL, Simpson E, Liu Y, Baucum AJ. A multi-omic analysis of the dorsal striatum in an animal model of divergent genetic risk for alcohol use disorder. *J Neurochem*. 2021;157:1013–1031. doi: 10.1111/jnc.15226
29. Mosley AL, Sardiu ME, Pattenden SG, Workman JL, Florens L, Washburn MP. Highly reproducible label free quantitative proteomic analysis of RNA polymerase complexes. *Mol Cell Proteomics*. 2011;10:S1–S13. doi: 10.1074/mcp.M110.000687
30. Ge SX, Jung D, Yao R. ShinyGO: a graphical gene-set enrichment tool for animals and plants. *Bioinformatics*. 2020;36:2628–2629. doi: 10.1093/bioinformatics/btz931
31. Denizli M, Capitano ML, Kua KL. Maternal obesity and the impact of associated early-life inflammation on long-term health of offspring. *Front Cellular Inf Mmicrobiol*. 2022;12:940937. doi: 10.3389/fcimb.2022.940937
32. Casasnovas J, Damron CL, Jarrell J, Orr KS, Bone RN, Archer-Hartmann S, Azadi P, Kua KL. Offspring of obese dams exhibit sex-differences in pancreatic heparan sulfate glycosaminoglycans and islet insulin secretion. *Front Endocrinol*. 2021;12:658439. doi: 10.3389/fendo.2021.658439
33. Krishnan A, Samtani R, Dhanantwari P, Lee E, Yamada S, Shiota K, Donofrio MT, Leatherbury L, Lo CW. A detailed comparison of mouse and human cardiac development. *Pediatric Res*. 2014;76:500–507. doi: 10.1038/pr.2014.128
34. Loeken M. Free radicals and birth defects. *J Matern Fetal Neonatal Med*. 2004;15:6–14.
35. VanDusen NJ, Vincentz JW, Firulli BA, Howard MJ, Rubart M, Firulli AB. Loss of Hand2 in a population of Periostin lineage cells results in pronounced bradycardia and neonatal death. *Develop Biol*. 2014;388:149–158. doi: 10.1016/j.ydbio.2014.02.010
36. Holler KL, Hendershot TJ, Troy SE, Vincentz JW, Firulli AB, Howard MJ. Targeted deletion of Hand2 in cardiac neural crest-derived cells influences cardiac gene expression and outflow tract development. *Develop Biol*. 2010;341:291–304. doi: 10.1016/j.ydbio.2010.02.001
37. Van Dusen NJ, Casanovas J, Vincentz JW, Firulli BA, Osterwalder M, Lopez-Rios J, Zeller R, Zhou B, Grego-Bessa J, De La Pompa JL. Hand2 is an essential regulator for two notch-dependent functions within the embryonic endocardium. *Cell Reports*. 2014;9:2071–2083.
38. Barnes RM, Firulli BA, VanDusen NJ, Morikawa Y, Conway SJ, Cserjesi P, Vincentz JW, Firulli AB. Hand2 loss-of-function in Hand1-expressing cells reveals distinct roles in epicardial and coronary vessel development. *Circul Res*. 2011;108:940–949.
39. Sheikh F, Lyon RC, Chen J. Functions of myosin light chain-2 (MYL2) in cardiac muscle and disease. *Gene*. 2015;569:14–20. doi: 10.1016/j.gene.2015.06.027
40. Singh CK, Chhabra G, Ndiaye MA, Garcia-Peterson LM, Mack NJ, Ahmad N. The role of sirtuins in antioxidant and redox signaling. *Antioxidants and Redox Signal*. 2018;28:643–661. doi: 10.1089/ars.2017.7290
41. Wek R, Jiang H-Y, Anthony T. Coping with stress: eIF2 kinases and translational control. *Biochem Soc Trans*. 2006;34(Pt 1):7–11. doi: 10.1042/BST20060007
42. Shi J, Wei L. Rho kinases in embryonic development and stem cell research. *Arch Immunol Ther Exp*. 2022;70:1–22.
43. Phillips HM, Mahendran P, Singh E, Anderson RH, Chaudhry B, Henderson DJ. Neural crest cells are required for correct positioning of the developing outflow cushions and pattern the arterial valve leaflets. *Cardiovasc Res*. 2013;99:452–460. doi: 10.1093/cvr/cvt132
44. Cai L, Kang YJ. Oxidative stress and diabetic cardiomyopathy: a brief review. *Cardiovasc Toxicol*. 2001;1:181–193. doi: 10.1385/CT:1:3:181
45. Yucel D, Aydogdu S, Cehreli S, Saydam G, Canatan H, Senes M, Topkaya BC, Nebioglu S. Increased oxidative stress in dilated cardiomyopathic heart failure. *Clini Chem*. 1998;44:148–154. doi: 10.1093/clinchem/44.1.148
46. Valavanidis A, Vlachogianni T, Fiotakis C. 8-hydroxy-2′-deoxyguanosine (8-OHdG): a critical biomarker of oxidative stress and carcinogenesis. *J Environ Sci Health Part C, Environ Toxicol Risk Assess*. 2009;27:120–139. doi: 10.1080/10590500902885684
47. Yuan Y, Zhang L, Jin L, Liu J, Li Z, Wang L, Ren A. Markers of macromolecular oxidative damage in maternal serum and risk of neural tube defects in offspring. *Free Radic Biol Med*. 2015;80:27–32. doi: 10.1016/j.freeradbiomed.2014.12.014
48. Nunes KP, Webb RC. New insights into RhoA/rho-kinase signaling: a key regulator of vascular contraction. *Small GTPases*. 2021;12:458–469. doi: 10.1080/21541248.2020.1822721
49. Sakurai A, Doci C, Gutkind JS. Semaphorin signaling in angiogenesis, lymphangiogenesis and cancer. *Cell Res*. 2012;22:23–32. doi: 10.1038/cr.2011.198
50. Sun Q, Liu S, Liu K, Jiao K. Role of semaphorin signaling during cardiovascular development. *J Am Heart Assoc*. 2018;7:e008853. doi: 10.1161/JAHA.118.008853
51. Sumi T, Matsumoto K, Takai Y, Nakamura T. Cofilin phosphorylation and actin cytoskeletal dynamics regulated by rho-and Cdc42-activated LIM-kinase 2. *J Cell Biol*. 1999;147:1519–1532. doi: 10.1083/jcb.147.7.1519
52. Pignataro M, Di Rocco G, Lancellotti L, Bernini F, Subramanian K, Castellini E, Bortolotti CA, Malferrari D, Moro D, Valdre G. Phosphorylated cofilin-2 is more prone to oxidative modifications on Cys39 and favors amyloid fibril formation. *Redox Biol*. 2020;37:101691.
53. Manzoni C, Kia DA, Vandrovcova J, Hardy J, Wood NW, Lewis PA, Ferrari R. Genome, transcriptome and proteome: the rise of omics data and their integration in biomedical sciences. *Briefing Bioinform*. 2018;19:286–302. doi: 10.1093/bib/bbw114
54. McGreevy EM, Vijayraghavan D, Davidson LA, Hildebrand JD. Shroom3 functions downstream of planar cell polarity to regulate myosin II distribution and cellular organization during neural tube closure. *Biol Open*. 2015;4:BIO20149589. doi: 10.1242/bio.20149589
55. Nishimura T, Takeichi M. Shroom3-mediated recruitment of rho kinases to the apical cell junctions regulates epithelial and neuroepithelial

planar remodeling. *Development*. 2008;135:1493–1502. doi: 10.1242/dev.019646
56. Simões SM, Mainieri A, Zallen JA. Rho GTPase and shroom direct planar polarized actomyosin contractility during convergent extension. *J Cell Biol*. 2014;204:575–589.
57. Nishimura T, Honda H, Takeichi M. Planar cell polarity links axes of spatial dynamics in neural-tube closure. *Cell*. 2012;149:1084–1097. doi: 10.1016/j.cell.2012.04.021
58. Ossipova O, Chuykin I, Chu C-W, Sokol SY. Vangl2 cooperates with Rab11 and myosin V to regulate apical constriction during vertebrate gastrulation. *Development*. 2015;142:99–107. doi: 10.1242/dev.111161
59. Kowalczyk I, Lee C, Schuster E, Hoeren J, Trivigno V, Riedel L, Görne J, Wallingford JB, Hammes A, Feistel K. Neural tube closure requires the endocytic receptor Lrp2 and its functional interaction with intracellular scaffolds. *Development*. 2021;148:dev195008. doi: 10.1242/dev.195008
60. Marean A, Graf A, Zhang Y, Niswander L. Folic acid supplementation can adversely affect murine neural tube closure and embryonic survival. *Hum Molecu Genet*. 2011;20:3678–3683. doi: 10.1093/hmg/ddr289
61. Xu C, Yang P. 1327-P: maternal diabetes suppresses neural tube closure gene Shroom3 through DNA hypermethylation and thus disrupts planar cell polarity. *Diabetes*. 2020;69(suppl 1):1327-P. doi: 10.2337/db20-1327-P
62. Durbin MD, O'Kane J, Lorentz S, Firulli AB, Ware SM. SHROOM3 is downstream of the planar cell polarity pathway and loss-of-function results in congenital heart defects. *Develop Biol*. 2020;464:124–136. doi: 10.1016/j.ydbio.2020.05.013
63. Lutz TA. Mammalian models of diabetes mellitus, with a focus on type 2 diabetes mellitus. *Nat Rev Endocrinol*. 2023;19:350–360. doi: 10.1038/s41574-023-00818-3
64. Clark DA, Banwatt D, Chaouat G. Stress-triggered abortion in mice prevented by alloimmunization. *Am J Reprod Immunol*. 1993;29:141–147. doi: 10.1111/j.1600-0897.1993.tb00579.x
65. van Vliet-Ostaptchouk J, den Hoed M, Luan J, Zhao J, Ong K, Van Der Most P, Wong A, Hardy R, Kuh D, Van Der Klauw M. Pleiotropic effects of obesity-susceptibility loci on metabolic traits: a meta-analysis of up to 37,874 individuals. *Diabetologia*. 2013;56:2134–2146.
66. Fernandez-Twinn DS, Blackmore HL, Siggens L, Giussani DA, Cross CM, Foo R, Ozanne SE. The programming of cardiac hypertrophy in the offspring by maternal obesity is associated with hyperinsulinemia, AKT, ERK, and mTOR activation. *Endocrinology*. 2012;153:5961–5971. doi: 10.1210/en.2012-1508
67. Almansa-Ordonez A, Bellido R, Vassena R, Barragan M, Zambelli F. Oxidative stress in reproduction: a mitochondrial perspective. *Biology*. 2020;9:269. doi: 10.3390/biology9090269
68. Hu C, Yang Y, Li J, Wang H, Cheng C, Yang L, Li Q, Deng J, Liang Z, Yin Y. Maternal diet-induced obesity compromises oxidative stress status and angiogenesis in the porcine placenta by upregulating Nox2 expression. *Oxidative Med Cell Longev*. 2019;1:2481592.
69. Dennery PA. Effects of oxidative stress on embryonic development. *Birth Defects Res C Embryo Today*. 2007;81:155–162. doi: 10.1002/bdrc.20098
70. Pantaleão LC, Inzani I, Furse S, Loche E, Hufnagel A, Ashmore T, Blackmore HL, Jenkins B, Carpenter AA, Wilczynska A. Maternal diet-induced obesity during pregnancy alters lipid supply to mouse E18. 5 fetuses and changes the cardiac tissue lipidome in a sex-dependent manner. *elife*. 2022;11:e69078.
71. Pantaleão LC, Loche E, Fernandez-Twinn DS, Dearden L, Córdova-Casanova A, Osmond C, Salonen MK, Kajantie E, Niu Y, de Almeida-Faria J. Programming of cardiac metabolism by miR-15b-5p, a miRNA released in cardiac extracellular vesicles following ischemia-reperfusion injury. *Mol Metab*. 2024;80:101875.
72. Wu Y, Reece EA, Zhong J, Dong D, Shen W-B, Harman CR, Yang P. Type 2 diabetes mellitus induces congenital heart defects in murine embryos by increasing oxidative stress, endoplasmic reticulum stress, and apoptosis. *Am J Obstet Gynecol*. 2016;215:366.e361–366.e310.
73. Wentzel P, Gareskog M, Eriksson UJ. Decreased cardiac glutathione peroxidase levels and enhanced mandibular apoptosis in malformed embryos of diabetic rats. *Diabetes*. 2008;57:3344–3352. doi: 10.2337/db08-0830
74. Sivan E, Lee YC, Wu YK, Reece EA. Free radical scavenging enzymes in fetal dysmorphogenesis among offspring of diabetic rats. *Teratology*. 1997;56:343–349. doi: 10.1002/(SICI)1096-9926
75. Yang P. Superoxide Dismutase 1 in vivo Ameliorates Maternal Diabetes-Induced Apoptosis and Heart Defects through Restoration of Impaired Wnt Signaling.
76. Dong D, Yu J, Wu Y, Fu N, Villela NA, Yang P. Maternal diabetes triggers DNA damage and DNA damage response in neurulation stage embryos through oxidative stress. *Biochem Biophys Res Commu*. 2015;467:407–412. doi: 10.1016/j.bbrc.2015.09.137
77. Costa-Mattioli M, Walter P. The integrated stress response: from mechanism to disease. *Science*. 2020;368:eaat5314. doi: 10.1126/science.aat5314
78. Wang X, Proud CG. The role of eIF2 phosphorylation in cell and organismal physiology: new roles for well-known actors. *Biochem J*. 2022;479:1059–1082. doi: 10.1042/BCJ20220068
79. Santos-Ribeiro D, Godinas L, Pilette C, Perros F. The integrated stress response system in cardiovascular disease. *Drug Discovery Today*. 2018;23:920–929. doi: 10.1016/j.drudis.2018.02.008
80. Prola A, Da Pires Silva J, Guilbert A, Lecru L, Piquereau J, Ribeiro M, Mateo P, Gressette M, Fortin D, Boursier C. SIRT1 protects the heart from ER stress-induced cell death through eIF2α deacetylation. *Cell Death Differ*. 2017;24:343–356. doi: 10.1038/cdd.2016.138
81. Hu C, Yan Y, Ji F, Zhou H. Maternal obesity increases oxidative stress in placenta and it is associated with intestinal microbiota. *Front Cell Infect Microbiol*. 2021;11:671347. doi: 10.3389/fcimb.2021.671347
82. Zhang CX, Candia AA, Sferruzzi-Perri AN. Placental inflammation, oxidative stress, and fetal outcomes in maternal obesity. *Trends Endocrinol Metab*. 2024;35:638–647. doi: 10.1016/j.tem.2024.02.002
83. Malti N, Merzouk H, Merzouk S, Loukidi B, Karaouzene N, Malti A, Narce M. Oxidative stress and maternal obesity: feto-placental unit interaction. *Placenta*. 2014;35:411–416. doi: 10.1016/j.placenta.2014.03.010
84. Soeda J, Mouralidarane A, Cordero P, Li J, Nguyen V, Carter R, Kapur SR, Pombo J, Poston L, Taylor PD. Maternal obesity alters endoplasmic reticulum homeostasis in offspring pancreas. *J Physiol Biochem*. 2016;72:281–291. doi: 10.1007/s13105-016-0476-6
85. Zhu S, Nguyen A, Pang J, Zhao J, Chen Z, Liang Z, Gu Y, Huynh H, Bao Y, Lee S. Mitochondrial stress induces an HRI-eIF2α pathway protective for cardiomyopathy. *Circulation*. 2022;146:1028–1031. doi: 10.1161/CIRCULATIONAHA.122.059594
86. Gaccioli F, White V, Capobianco E, Powell TL, Jawerbaum A, Jansson T. Maternal overweight induced by a diet with high content of saturated fat activates placental mTOR and eIF2alpha signaling and increases fetal growth in rats. *Biol Reprod*. 2013;89:91.
87. Shi J, Wei L. Rho kinases in cardiovascular physiology and pathophysiology: the effect of fasudil. *J Cardiovasc Pharmacol*. 2013;62:341–354. doi: 10.1097/FJC.0b013e3182a3718f
88. Zhao Z, Rivkees SA. Rho-associated kinases play an essential role in cardiac morphogenesis and cardiomyocyte proliferation. *Devel Dynamics: An Offic Public Am Assoc Anatomists*. 2003;226:24–32. doi: 10.1002/dvdy.10212
89. Schlessinger K, Hall A, Tolwinski N. Wnt signaling pathways meet rho GTPases. *Genes Devel*. 2009;23:265–277. doi: 10.1101/gad.1760809
90. Semenov MV, Habas R, MacDonald BT, He X. SnapShot: noncanonical Wnt signaling pathways. *Cell*. 2007;131:1378. doi: 10.1016/j.cell.2007.12.011
91. Phillips HM, Murdoch JN, Chaudhry B, Copp AJ, Henderson DJ. Vangl2 acts via RhoA signaling to regulate polarized cell movements during development of the proximal outflow tract. *Circul Res*. 2005;96:292–299.
92. Schleiffarth JR, Person AD, Martinsen BJ, Sukovich DJ, Neumann A, Baker CV, Lohr JL, Cornfield DN, Ekker SC, Petryk A. Wnt5a is required for cardiac outflow tract septation in mice. *Pediatric Res*. 2007;61:386.
93. Nagy II, Railo A, Rapila R, Hast T, Sormunen R, Tavi P, Räsänen J, Vainio SJ. Wnt-11 signalling controls ventricular myocardium development by patterning N-cadherin and β-catenin expression. *Cardiovasc Res*. 2009;85:100–109.
94. Henderson DJ, Conway SJ, Greene ND, Gerrelli D, Murdoch JN, Anderson RH, Copp AJ. Cardiovascular defects associated with abnormalities in midline development in the loop-tail mouse mutant. *Circ Res*. 2001;89:6–12. doi: 10.1161/hh1301.092497
95. Phillips HM, Rhee HJ, Murdoch JN, Hildreth V, Peat JD, Anderson RH, Copp AJ, Chaudhry B, Henderson DJ. Disruption of planar cell polarity signaling results in congenital heart defects and cardiomyopathy attributable to early cardiomyocyte disorganization. *Circul Res*. 2007;101:137–145. doi: 10.1161/CIRCRESAHA.106.142406

96. Hamblet NS, Lijam N, Ruiz-Lozano P, Wang J, Yang Y, Luo Z, Mei L, Chien KR, Sussman DJ, Wynshaw-Boris A. Dishevelled 2 is essential for cardiac outflow tract development, somite segmentation and neural tube closure. *Development*. 2002;129:5827–5838.
97. Etheridge SL, Ray S, Li S, Hamblet NS, Lijam N, Tsang M, Greer J, Kardos N, Wang J, Sussman DJ. Murine dishevelled 3 functions in redundant pathways with dishevelled 1 and 2 in normal cardiac outflow tract, cochlea, and neural tube development. *PLoS Genet*. 2008;4:e1000259. doi: 10.1371/journal.pgen.1000259
98. Curtin JA, Quint E, Tsipouri V, Arkell RM, Cattanach B, Copp AJ, Henderson DJ, Spurr N, Stanier P, Fisher EM. Mutation of Celsr1 disrupts planar polarity of inner ear hair cells and causes severe neural tube defects in the mouse. *Curr Biol*. 2003;13:1129–1133. doi: 10.1016/S0960-9822(03)00374-9
99. Zhou W, Lin L, Majumdar A, Li X, Zhang X, Liu W, Etheridge L, Shi Y, Martin J, Van de Ven W. Modulation of morphogenesis by noncanonical Wnt signaling requires ATF/CREB family–mediated transcriptional activation of TGFβ2. *Nat Geneti*. 2007;39:1225.
100. Yu H, Smallwood PM, Wang Y, Vidaltamayo R, Reed R, Nathans J. Frizzled 1 and frizzled 2 genes function in palate, ventricular septum and neural tube closure: general implications for tissue fusion processes. *Development*. 2010;137:3707–3717. doi: 10.1242/dev.052001
101. Paudyal A, Damrau C, Patterson VL, Ermakov A, Formstone C, Lalanne Z, Wells S, Lu X, Norris DP, Dean CH. The novel mouse mutant, chuzhoi, has disruption of Ptk7 protein and exhibits defects in neural tube, heart and lung development and abnormal planar cell polarity in the ear. *BMC Devel Biol*. 2010;10:87. doi: 10.1186/1471-213X-10-87
102. Fuster JJ, Zuriaga MA, Ngo DT-M, Farb MG, Aprahamian T, Yamaguchi TP, Gokce N, Walsh K. Noncanonical Wnt signaling promotes obesity-induced adipose tissue inflammation and metabolic dysfunction independent of adipose tissue expansion. *Diabetes*. 2015;64:1235–1248. doi: 10.2337/db14-1164
103. Zuriaga MA, Fuster JJ, Farb MG, MacLauchlan S, Bretón-Romero R, Karki S, Hess DT, Apovian CM, Hamburg NM, Gokce N. Activation of non-canonical WNT signaling in human visceral adipose tissue contributes to local and systemic inflammation. *Scientific Rep*. 2017;7:17326. doi: 10.1038/s41598-017-17509-5
104. Catalán V, Gómez-Ambrosi J, Rodríguez A, Pérez-Hernández AI, Gurbindo J, Ramírez B, Méndez-Giménez L, Rotellar F, Valentí V, Moncada R. Activation of noncanonical Wnt signaling through WNT5A in visceral adipose tissue of obese subjects is related to inflammation. *J Clin Endocrinol Metabol*. 2014;99:E1407–E1417. doi: 10.1210/jc.2014-1191
105. Schulte DM, Müller N, Neumann K, Oberhäuser F, Faust M, Güdelhöfer H, Brandt B, Krone W, Laudes M. Pro-inflammatory wnt5a and anti-inflammatory sFRP5 are differentially regulated by nutritional factors in obese human subjects. *PloS One*. 2012;7:e32437. doi: 10.1371/journal.pone.0032437
106. Coleman ML, Sahai EA, Yeo M, Bosch M, Dewar A, Olson MF. Membrane blebbing during apoptosis results from caspase-mediated activation of ROCK I. *Nat Cell Biol*. 2001;3:339–345.
107. Sapet C, Simoncini S, Loriod B, Puthier D, Sampol J, Nguyen C, Dignat-George F, Anfosso F. Thrombin-induced endothelial microparticle generation: identification of a novel pathway involving ROCK-II activation by caspase-2. *Blood*. 2006;108:1868–1876. doi: 10.1182/blood-2006-04-014175
108. Tosello-Trampont A-C, Nakada-Tsukui K, Ravichandran KS. Engulfment of apoptotic cells is negatively regulated by rho-mediated signaling. *J Biol Chem*. 2003;278:49911–49919. doi: 10.1074/jbc.M306079200
109. Moore M, Marroquin BA, Gugliotta W, Tse R, White SR. Rho kinase inhibition initiates apoptosis in human airway epithelial cells. *Am J Resp Cell Molecu Biol*. 2004;30:379–387. doi: 10.1165/rcmb.2003-0019OC
110. Özdemir A, İbişoğlu B, Demir YDŞ, Benhür E, Valipour F, Ark M. A novel proteolytic cleavage of ROCK 1 in cell death: not only by caspases 3 and 7 but also by caspase 2. *Biochem Biophys Res Commun*. 2021;547:118–124.
111. Patel R, Sriramoji S, Marucci M, Aziz I, Shah S, Sesti F. Cytoskeletal remodeling via rho GTPases during oxidative and thermal stress in Caenorhabditis elegans. *Biochem Biophys Res Commu*. 2017;492:338–342. doi: 10.1016/j.bbrc.2017.08.112
112. Karki P, Birukov KG. Rho and reactive oxygen species at crossroads of endothelial permeability and inflammation. *Antioxidants and Redox Signal*. 2019;31:1009–1022. doi: 10.1089/ars.2019.7798
113. Okashah S, Vasudeva D, El Jerbi A, Khodjet-El-khil H, Al-Shafai M, Syed N, Kambouris M, Udassi S, Saraiva LR, Al-Saloos H. Investigation of genetic causes in patients with congenital heart disease in Qatar: findings from the Sidra cardiac registry. *Gene*. 2022;13:1369.
114. Tariq M, Belmont JW, Lalani S, Smolarek T, Ware SM. SHROOM3 is a novel candidate for heterotaxy identified by whole exome sequencing. *Genome Biol*. 2011;12:R91. doi: 10.1186/gb-2011-12-9-r91
115. Calcagno D, Taghdiri N, Ninh V, Mesfin J, Toomu A, Sehgal R, Lee J, Liang Y, Duran J, Adler E. Single-cell and spatial transcriptomics of the infarcted heart define the dynamic onset of the border zone in response to mechanical destabilization. *Nature Cardiovasc Res*. 2022;1:1039–1055.
116. Blackmore HL, Niu Y, Fernandez-Twinn DS, Tarry-Adkins JL, Giussani DA, Ozanne SE. Maternal diet-induced obesity programs cardiovascular dysfunction in adult male mouse offspring independent of current body weight. *Endocrinology*. 2014;155:3970–3980. doi: 10.1210/en.2014-1383
117. Loche E, Blackmore HL, Carpenter AA, Beeson JH, Pinnock A, Ashmore TJ, Aiken CE, de Almeida-Faria J, Schoonejans JM, Giussani DA. Maternal diet-induced obesity programmes cardiac dysfunction in male mice independently of post-weaning diet. *Cardiovasc Res*. 2018;114:1372–1384.
118. Puente BN, Kimura W, Muralidhar SA, Moon J, Amatruda JF, Phelps KL, Grinsfelder D, Rothermel BA, Chen R, Garcia JA. The oxygen-rich postnatal environment induces cardiomyocyte cell-cycle arrest through DNA damage response. *Cell*. 2014;157:565–579.
119. Francou A, De Bono C, Kelly RG. Epithelial tension in the second heart field promotes mouse heart tube elongation. *Nat Commun*. 2017;8:14770. doi: 10.1038/ncomms14770
120. van den Berg G, Abu-Issa R, de Boer BA, Hutson MR, de Boer PA, Soufan AT, Ruijter JM, Kirby ML, van den Hoff MJ, Moorman AF. A caudal proliferating growth center contributes to both poles of the forming heart tube. *Circul Res*. 2009;104:179–188. doi: 10.1161/CIRCRESAHA.108.185843
121. Sinha T, Wang B, Evans S, Wynshaw-Boris A, Wang J. Disheveled mediated planar cell polarity signaling is required in the second heart field lineage for outflow tract morphogenesis. *Develop Biol*. 2012;370:135–144. doi: 10.1016/j.ydbio.2012.07.023
122. Schlüter K-D, Kutsche HS, Hirschhäuser C, Schreckenberg R, Schulz R. Review on chamber-specific differences in right and left heart reactive oxygen species handling. *Front Physiol*. 2018;9:423506.
123. Brown E, Heerspink HJ, Cuthbertson DJ, Wilding JP. SGLT2 inhibitors and GLP-1 receptor agonists: established and emerging indications. *Lancet*. 2021;398:262–276. doi: 10.1016/S0140-6736(21)00536-5
124. Wang F, Reece EA, Yang P. Superoxide dismutase 1 overexpression in mice abolishes maternal diabetes–induced endoplasmic reticulum stress in diabetic embryopathy. *Am J Obstet Gynecol*. 2013;209:345.e341–345.e347.
125. Choudhury TZ, Greskovich SC, Girard HB, Rao AS, Budhathoki Y, Cameron EM, Conroy S, Li D, Zhao M-T, Garg V. Impact of genetic factors on antioxidant rescue of maternal diabetes–associated congenital heart disease. *JCI Insight*. 2024;9:e183516. doi: 10.1172/jci.insight.183516